Mon. Not. R. Astron. Soc. **000**, 1–18 (2014) Printed 18 February 2015 (MN LaTeX style file v2.2)

Massive stars exploding in a He-rich circumstellar medium. IV. Transitional Type Ibn Supernovae

A. Pastorello,[1⋆] S. Benetti,[1] P. J. Brown,[2] D. Y. Tsvetkov,[3] C. Inserra,[4] S. Taubenberger,[6] L. Tomasella,[1] M. Fraser,[5] D. J. Rich,[7] M. T. Botticella,[8] F. Bufano,[9] E. Cappellaro,[1] M. Ergon,[10] E. S. Gorbovskoy,[3,11] A. Harutyunyan,[12] F. Huang,[13,14] R. Kotak,[4] V. M. Lipunov,[3,11] L. Magill,[4] M. Miluzio,[1,15] N. Morrell,[16] P. Ochner,[1] S. J. Smartt,[4] J. Sollerman,[10] S. Spiro,[1,17] M. D. Stritzinger,[18] M. Turatto,[1] S. Valenti,[19,20] X. Wang,[14] D. E. Wright,[4] V. V. Yurkov,[21] L. Zampieri,[1] and T. Zhang.[22]

[1] *INAF-Osservatorio Astronomico di Padova, Vicolo dell'Osservatorio 5, 35122 Padova, Italy*
[2] *George P. and Cynthia Woods Mitchell Institute for Fundamental Physics & Astronomy, Texas A. & M. University, Department of Physics and Astronomy, 4242 TAMU, College Station, TX 77843, USA*
[3] *Sternberg Astronomical Institute of Lomonosov Moscow State University, University Avenue 13, 119992 Moscow, Russia*
[4] *Astrophysics Research Centre, School of Mathematics and Physics, Queen's University Belfast, Belfast BT7 1NN, United Kingdom*
[5] *Institute of Astronomy, University of Cambridge, Madingley Road, Cambridge, CB3 0HA, United Kingdom*
[6] *Max-Planck-Institut für Astrophysik, Karl-Schwarzschild-Str. 1, 85741 Garching, Germany*
[7] *Rich Observatory, 62 Wessnette Dr., Hampden, ME, USA*
[8] *INAF - Osservatorio Astronomico d Capodimonte, Salita Moiariello 16, 80131 Napoli, Italy*
[9] *Departamento de Ciencias Fisicas, Universidad Andres Bello, Avda. Republica 252, Santiago, Santiago RM, Chile*
[10] *Department of Astronomy, The Oskar Klein Centre, Stockholm University, 106 91 Stockholm, Sweden*
[11] *Lomonosov Moscow State University, GSP-1, Leninskie Gory, Moscow, 119991, Russia*
[12] *Fundación Galileo Galilei-INAF, Telescopio Nazionale Galileo, Rambla Jos Ana Fernández Pérez 7, 38712 Breña Baja, TF, Spain*
[13] *Department of Astronomy, Beijing Normal University, Beijing, 100875, China*
[14] *Physics Department and Tsinghua Center for Astrophysics, Tsinghua University, Beijing, 100084, China*
[15] *Dipartimento di Astronomia, Universitá di Padova, Vicolo dellOsservatorio 3, 35122 Padova, Italy*
[16] *Carnegie Observatories, Las Campanas Observatory, Colina El Pino, Casilla 601, Chile*
[17] *Department of Physics (Astrophysics), University of Oxford, DWB, Keble Road, Oxford OX1 3RH, United Kingdom*
[18] *Department of Physics and Astronomy, Aarhus University, Ny Munkegade, DK-8000 Aarhus C, Denmark*
[19] *Las Cumbres Observatory Global Telescope Network, Inc. Santa Barbara, CA 93117, USA*
[20] *Department of Physics, University of California Santa Barbara, Santa Barbara, CA 93106-9530, USA*
[21] *Blagoveshchensk State Pedagogical University, ul. Lenina 104, 675000 Blagoveshchensk, Russia*
[22] *National Astronomical Observatory of China, Chinese Academy of Sciences, Beijing, 100012, China*

Accepted 20XX Month XX. Received 20XX Month XX; in original form 20XX Month XX

arXiv:1502.04946v1 [astro-ph.SR] 17 Feb 2015

© 2014 RAS

ABSTRACT

We present ultraviolet, optical and near-infrared data of the Type Ibn supernovae (SNe) 2010al and 2011hw. SN 2010al reaches an absolute magnitude at peak of $M_R = -18.86 \pm 0.21$. Its early light curve shows similarities with normal SNe Ib, with a rise to maximum slower than most SNe Ibn. The spectra are dominated by a blue continuum at early stages, with narrow P-Cygni He I lines indicating the presence of a slow-moving, He-rich circumstellar medium. At later epochs the spectra well match those of the prototypical SN Ibn 2006jc, although the broader lines suggest that a significant amount of He was still present in the stellar envelope at the time of the explosion. SN 2011hw is somewhat different. It was discovered after the first maximum, but the light curve shows a double-peak. The absolute magnitude at discovery is similar to that of the second peak ($M_R = -18.59 \pm 0.25$), and slightly fainter than the average of SNe Ibn. Though the spectra of SN 2011hw are similar to those of SN 2006jc, coronal lines and narrow Balmer lines are cleary detected. This indicates substantial interaction of the SN ejecta with He-rich, but not H-free, circumstellar material. The spectra of SN 2011hw suggest that it is a transitional SN Ibn/IIn event similar to SN 2005la. While for SN 2010al the spectro-photometric evolution favours a H-deprived Wolf-Rayet progenitor (of WN-type), we agree with the conclusion of Smith et al. (2012) that the precursor of SN 2011hw was likely in transition from a luminous blue variable to an early Wolf-Rayet (Ofpe/WN9) stage.

Key words: supernovae: general — supernovae: individual (SN 2010al, SN 2011hw, SN 2006jc, SN 2005la, SN 2000er)

1 INTRODUCTION

Type Ibn supernovae (SNe) are a poorly understood family of core-collapse SNe (CC SNe). The label "SNe Ibn" was introduced a few years ago (Pastorello et al. 2008a), although the first object of this class was discovered almost a decade before (SN 1999cq, Matheson et al. 2000). Early spectra of SNe Ibn are blue, and show simultaneously broad lines of intermediate mass elements (IME) and relatively narrow lines of He, while lines of H are weak or absent. The lack of narrow Balmer lines is an observational property distinguishing this sub-group from classical Type IIn SNe. Although SNe Ibn are quite luminous, their photometric evolution is usually very rapid, with a very fast rise to maximum and a fast post-peak decline, at least in the optical bands. The latter has been proposed to be a signature of relatively early dust formation in a cool dense shell formed in the post-shock circumstellar medium (CSM; see e.g. Smith et al. 2008; Mattila et al. 2008). SNe Ibn are generally interpreted as Type Ib/c SN explosions occurring within a He-rich circumstellar environment.

The prototype of Type Ibn events is SN 2006jc, the first CC SN observed to explode a short time (2 yrs) after a major eruptive episode of the progenitor registered by the amateur astronomer K. Itagaki (Pastorello et al. 2007). Unfortunately SN 2006jc was discovered a few weeks after explosion, and we could not follow the early-time evolution. Nevertheless, whilst high-quality data are available in the literature for SN 2006jc[1], for other Type Ibn SNe only sparse optical data have been published (e.g. Matheson et al. 2000; Pastorello et al. 2008a,b).

Among recent additions to this family, remarkable objects are: PS1-12sk, iPFT13beo, LSQ12btw, LSQ13ccw and OGLE-2012-SN-006. PS1-12sk was discovered by the Pan-STARRS1 survey (Kaiser et al. 2002) and has been proposed to be the first Type Ibn SN hosted in an elliptical galaxy (Sanders et al. 2013). iPTF13beo is an intermediate Palomar Transient Factory (iPTF, Kulkarni 2013) discovery. It was detected soon after the explosion, and it showed a sort of double-peaked light curve (Gorbikov et al. 2014). LSQ12btw and LSQ13ccw are two objects discovered by the la Silla-Quest survey (Rabinowitz et al. 2011) and classified by the "Public ESO Spectroscopic Survey of Transient Objects" (PESSTO, Valenti et al. 2012; Kargas et al. 2013). The data of these two transients are presented in Pastorello et al. (2015a). OGLE-2012-SN-006 was discovered by the OGLE IV survey (Wyrzykowski et al. 2012) and classified as a Type Ibn SN a few months later (Prieto & Morrell 2013). This is the first SN Ibn with a slowly evolving late-time optical light curve (Pastorello et al. 2015b).

The first opportunity of a complete monitoring of a Type Ibn SN starting soon after explosion was provided with the discovery of SN 2010al in the spiral galaxy UGC 4286 on March 13, 2010 (Rich 2010). Early-time spectra showed some resemblance with those of the Type IIn SNe 1998S and 2001fa, and with early spectra of the Type II SN 1983K, for the detection of narrow H Balmer lines in emission and the presence of narrow features usually found in Wolf-Rayet winds, such as the N III / C III blend at 4640 Å and the He II λ4686 and λ5412 lines (Cooke et al. 2010; Stritzinger et al.

⋆ andrea.pastorello@oapd.inaf.it

[1] Multi-wavelength observations of SN 2006jc have been presented by Pastorello et al. (2007); Foley et al. (2007); Immler et al. (2008); Smith et al. (2008); Pastorello et al. (2008a); Mattila et al. (2008); Tominaga et al. (2008); Di Carlo et al. (2008); Nozawa et al. (2008); Sakon et al. (2009); Anupama et al. (2009); Bufano et al. (2009); Modjaz et al. (2014); Bianco et al. (2014).

2010; Silverman et al. 2010). However, the disappearance of H lines and the strengthening of He I features at later phases (see Section 4) suggest us to revise the classification of SN 2010al as a Type Ibn event. Two XShooter spectra of SN 2010al have been presented in Pastorello et al. (2012).

More recently, another interesting transient named SN 2011hw was discovered by B. Dintinjana and H. Mikuz (Crni Vrh Observatory) and classified by our team (Valenti et al. 2011). The object appeared to be similar to the transitional Type-IIn/Ibn SN 2005la (Pastorello et al. 2008b) because of the presence of H lines in emission, though weaker than the most prominent He I emission features (Dintinjana et al. 2011; Valenti et al. 2011). Sparse photometry and a nice spectral sequence of SN 2011hw have been presented by Smith et al. (2012), together with a comprehensive discussion on the nature of this transitional event.

In this paper we will present and analyse new data of the Type Ibn SNe 2010al and 2011hw collected in the framework of an extensive international collaboration assembled on the ESO-NTT and TNG *Supernova Variety and Nucleosynthesis Yields* Large programs.[2] In Section 2 we will present the observations of the two SNe. In Section 3 we will describe the photometric data reduction techniques and discuss the light curves of SNe 2010al and 2011hw. Spectroscopic data will be illustrated and analysed in Section 4. Finally, a discussion and a summary will follow in Section 5.

2 OBSERVATIONS

We started our optical and near-infrared (NIR) observational campaigns soon after the classification announcements of the two SNe, using the instruments available to our collaboration: the 8.2-m Very Large Telescope (VLT - UT2 module) with XShooter (Cerro Paranal, Chile); the 3.58-m New Technology Telescope (NTT) equipped with EFOSC2 and SOFI (La Silla, Chile); the 1.82-m Copernico Telescope with AFOSC and the 67/92-cm Schmidt Telescope (Mt. Ekar, near Asiago, Italy); the 2.2-m telescope in Calar Alto (Almeria, Spain) with CAFOS; the two 0.40-m MASTER telescopes[3] in Kislovodsk (Caucasian region, Russia) and Blagoveschensk (Far East region, Russia) both equipped with Apogee Alta U16M CCDs; the 2.0-m Faulkes North telescope with the EM01 camera (Haleakala, Hawaii Islands, USA); the 0.80-m Tsinghua-NAOC (National Astronomical Observatories of China) Telescope (Xinglong Observatory, Yanshan mountains, Hebei, China), equipped with a Princeton Instruments VersArray:1300B CCD; the 3.58-m Telescopio Nazionale Galileo (TNG) with Dolores and NICS; the 4.2-m William Herschel Telescope (WHT) equipped with ACAM and ISIS; the 2.0-m Liverpool Telescope (LT) with RATCam and SupIRCam; the 2.56m Nordic Optical Telescope (NOT) with ALFOSC (La Palma, Canary Islands, Spain). Additional photometry with small-size telescopes was kindly provided by amateur astronomers. Both SNe 2010al and 2011hw were visible for only 60-70 days after their discoveries, then they disappeared behind the Sun.

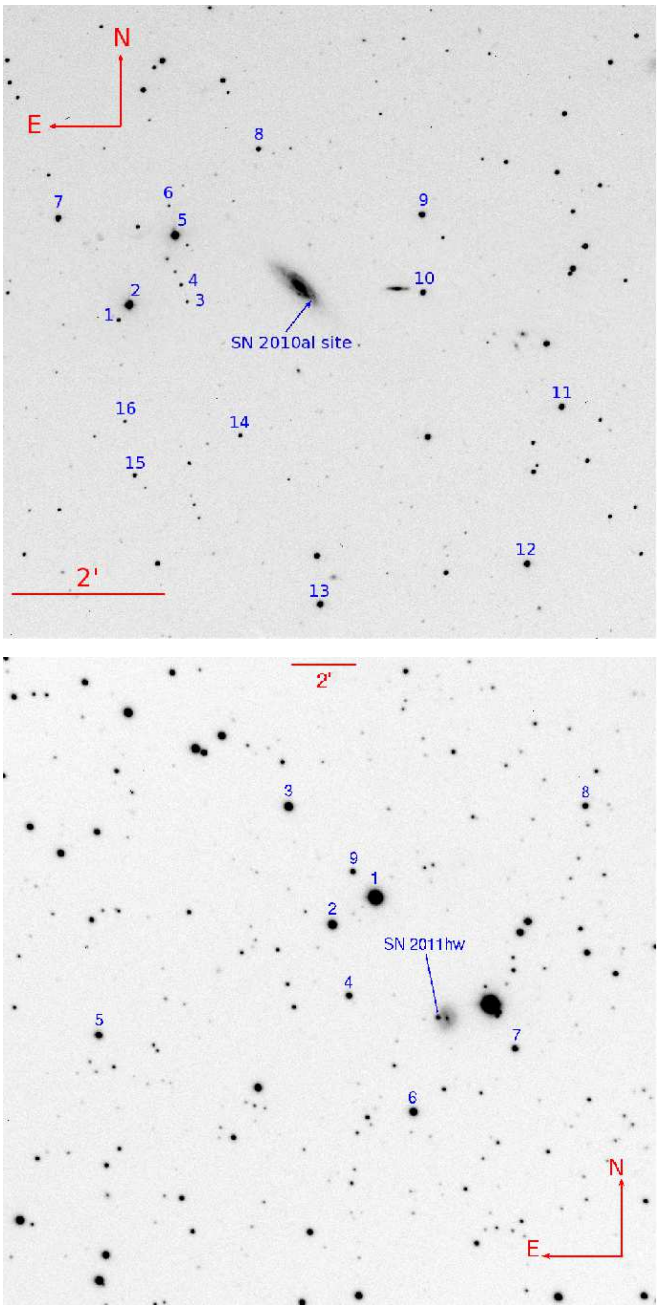

Figure 1. *R*-band images of the fields of SNe 2010al (**top**) and 2011hw (**bottom**). The sequence stars used to calibrate the magnitudes of the two SNe are marked.

We tried to recover SN 2010al at very late phases, but it was only visible in NIR observations obtained with the 8.4-m Large Binocular Telescope (Mt. Graham, Arizona; USA) equipped with Lucifer. Additional space observations of SNe 2010al and 2011hw in the ultra-violet (UV) and optical bands were obtained with the SWIFT satellite and its Ultra-violet/Optical Telescope (UVOT). These data were useful to

[2] *http://sngroup.oapd.inaf.it/esolarge.html*
[3] Information on the genesis and management of the Master Network can be found in Lipunov et al. (2010) and Kornilov et al. (2012).

constrain the large energy contribution of the UV domain in the early phases of the evolution of the two SNe.[4]

3 PHOTOMETRY

3.1 Data reduction

Data reduction was performed following standard prescriptions in IRAF.[5] Original images were first overscan-, bias-, flat field- and fringing-corrected, and then the unexposed regions of the images were trimmed. Occasionally, in order to increase the signal-to-noise ratio, several subsequent exposures were combined.

In order to remove the contribution of the bright background in the NIR images, we subtracted from individual science frames adjacent sky images, and then we combined the sky-subtracted SN exposures. The sky images were obtained by median-combining several dithered exposures of stellar regions in the proximity of the SN location.

The SN magnitudes were measured using a point spread function (PSF) fitting technique. Photometric zero-points and colour terms were obtained through observations of standard star fields in the same nights as the SN observations. The photometric calibrations in the optical domain were based on the Landolt (1992) catalogue. The inferred zero-points allowed us to calibrate the magnitudes of local stellar sequences in the fields of the two SNe (cfr. Figure 1 and Table A1). For non-photometric nights, we applied zero-point corrections derived by comparing the magnitudes of the local sequence stars of those nights with the average magnitudes obtained using a few photometric nights. With the corrected zero-points we estimated the final SN apparent magnitudes (Tables A3 and A4) at all epochs. The calibration of the NIR photometry of SN 2010al was performed with respect to the 2MASS catalogue magnitudes (Skrutskie et al. 2006) of the same local stellar sequence used for the optical photometry, and the final NIR SN magnitudes are also reported in Table A3.

In addition to the ground-based observations, UV and optical follow-up observations for both SNe were obtained using the Swift satellite[6] equipped with UVOT (Roming et al. 2005; Poole et al. 2008). The data of these two SNe have been presented in Pritchard et al. (2014); here we perform independent measurements on the same dataset. UVOT photometry was performed following the method detailed in Brown et al. (2009). Since images without the SN were available in the cases of SNe 2010al and 2011hw, the template subtraction method was applied to remove the host galaxies and hence improve the photometric measurements (obtained using a 3 to 5 arcsec aperture). We note that no template subtraction was applied in the photometry presented by Pritchard et al. (2014). Optimised zero-points from Breeveld et al. (2011) were then used to convert count rates to the final UVOT magnitudes.[7] The UV magnitudes of a few reference stars in the fields of the two SNe are reported in Table A2.

3.2 Distance and reddening estimates

The location of SN 2010al is $RA = 8^h14^m15^s.91, Dec = +18^o26'18''.2$ (equinox J2000.0), 9.5 arcsec West and 8.1 arcsec South of the center of UGC 4286, an edge-on Sab-type spiral galaxy (Rich 2010, see also Figure 1, top). Its recessional velocity [8] corrected for Virgo infall is $v_{Vir} = 5157$ km s^{-1}. Adopting as Hubble constant $H_0 = 73$ km s^{-1} Mpc^{-1} ($\Omega_M = 0.27$, $\Omega_\Lambda = 0.73$), we obtain a luminosity distance of about 71.6 Mpc (corresponding to a distance modulus $\mu = 34.27 \pm 0.16$ mag). The Galactic interstellar absorption is estimated to be A_B(MW) = 0.17 mag (Schlafly & Finkbeiner 2011). In order to estimate the host galaxy contribution to the total reddening, we inspected our higher resolution XShooter spectra (see Section 4.1). The two lines of the Na I doublet (Na ID) are visible and deblended both at z=0 and at the host galaxy reshift. We note that the ratio between the equivalent widths (EWs) of the Na I lines of the host galaxy and the Galactic component is 0.43. Assuming the same dust to gas ratio and similar dust properties in the Galaxy and in UGC 4286, we can reasonably estimate that the host galaxy contribution to the reddening is lower (by a factor 0.43) than the Galactic contribution, i.e. A_B(host) = 0.07 mag. Therefore, hereafter, we will adopt for SN 2010al a total line-of-sight extinction of A_B(tot) = 0.24 mag in the B band.

SN 2011hw is located at $RA = 22^h26^m14^s.54, Dec = +34^o12'59''.1$ (equinox J2000.0), approximately 8 arcsec East and 1 arcsec North of the center of an anonymous host galaxy (Dintinjana et al. 2011), which is not listed in the major galaxy catalogues (Figure 1, bottom). The only way to estimate its distance is through the redshift as deduced from the shift of the SN spectral features. Valenti et al. (2011) determined a redshift of $z = 0.023 \pm 0.001$; a similar value was estimated by Smith et al. (2012). Assuming $H_0 = 73$ km s^{-1} Mpc^{-1} ($\Omega_M = 0.27$ and $\Omega_\Lambda = 0.73$), we obtain a luminosity distance of 96.2 Mpc, which implies $\mu = 34.92 \pm 0.24$ mag. Schlafly & Finkbeiner (2011) estimate a Milky Way contribution to the extinction of A_B(MW) = 0.42 mag. Since available spectra do not show any evident narrow interstellar line at the host galaxy rest frame, we assume that there is no host galaxy contribution to the total reddening. Therefore A_B(tot) = A_B(MW) = 0.42 mag.

3.3 Light Curves

The two SNe have different pre-discovery histories. SN 2010al was discovered on 2010 Mar 13.03 UT (JD = 2455268.53) and nothing was visible at the SN position in archive images obtained on 2010 Feb 7.12 UT (JD = 2455234.62, Rich 2010). This detection limit alone cannot constrain well the explosion epoch. However, pre-discovery

[4] SN 2010al was also targeted by the Hubble Space Telescope in the UV domain, at almost the same epochs as our X-Shooter spectra (Kirshner et al. 2010).

[5] IRAF is distributed by the National Optical Astronomy Observatory, which is operated by the Association of Universities for Research in Astronomy (AURA) under cooperative agreement with the National Science Foundation.

[6] Proposal PIs: P. J. Brown; T. Prichard; A. M. Soderberg

[7] Updated UVOT calibration files (released on January 18, 2013) were collected from the Swift Calibration Database: *http://heasarc.gsfc.nasa.gov/docs/heasarc/caldb/swift/*.

[8] from Hyperleda, *http://leda.univ-lyon1.fr/*

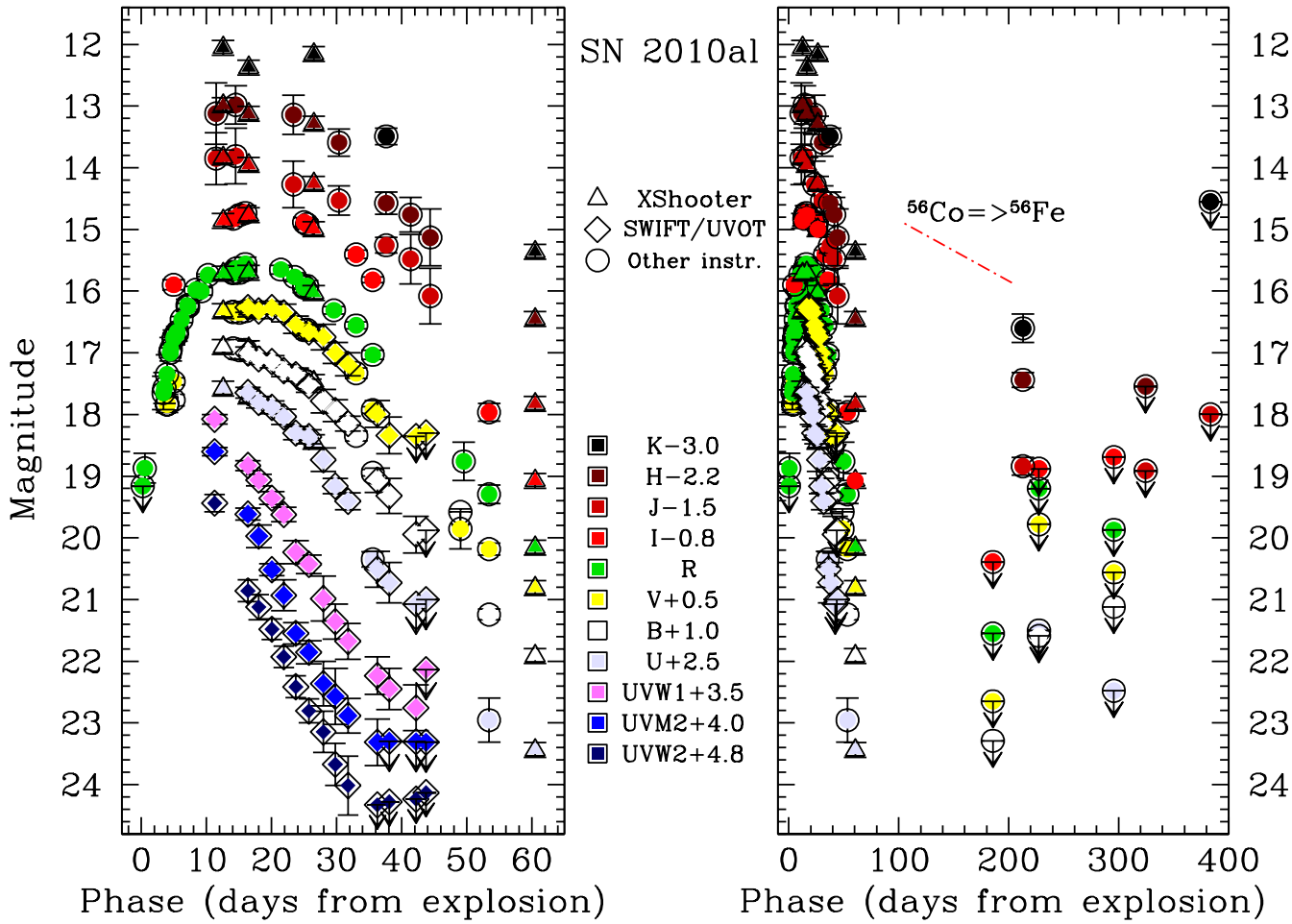

Figure 2. Left: Early-epoch UV (Swift/UVOT) + optical + NIR light curves of SN 2010al. The spectro-photometric points obtained from the XShooter spectra have also been included (see Tab. A3). Only significant detection limits have been shown in the figure. **Right:** optical + NIR light curves of SN 2010al, including late-time observations. Spectro-photometric observations with XShooter are indicated with triangles, SWIFT/UVOT data with diamonds, and data obtained with other instruments with circles. Different colours identify different photometric bands. Swift/UVOT optical-band magnitudes have been shifted by +0.082 mag in U, +0.026 mag in B and −0.037 mag in V to match the ground-based photometry. The light curve decline rate expected from the ^{56}Co to ^{56}Ni decay is also shown to guide the eye.

images obtained on Mar 12.71 UT (JD = 2455268.21) during routine observations performed with the 0.4-m MASTER telescope at Kislovodsk (Caucasian region, Russia) do not show any evidence of the SN to a limiting magnitude of R = 19.2. The fast rise of the light curve (see below) and the early spectra (Section 4) confirm that the object was discovered very young, close to the core-collapse epoch. Hereafter, we will adopt JD = 2455268.0 ± 1.5 as the time of the explosion.

On the contrary, the explosion epoch of SN 2011hw is not well known. Dintinjana et al. (2011) discovered SN 2011hw on 2011 Nov 18.72 UT (JD = 2455884.22), at an apparent unfiltered magnitude of 15.7. Our earliest follow-up observation was obtained one day after the discovery, and the SN magnitude was estimated to be R ≈ 16.6, i.e. almost 1 mag fainter than the magnitude reported by Dintinjana et al. (2011). We note that our photometry data are in decent agreement (within a few tenths mag) with those of Smith et al. (2012). The last prediscovery image with negative detection was on 2010 Dec 12 (with a limiting magnitude of 19.5), almost one year before (Dintinjana et al. 2011) and then does not tightly constrain the explosion epoch. However, a comparison of the first spectrum of SN 2011hw with the spectra of other Type Ibn SNe suggests that SN 2011hw was discovered quite late (see Section 4), at least a couple of weeks after the core-collapse. We adopt November 4th, 2011 (JD = 2455870 ± 10) as the epoch of the explosion.

SN 2010al has been extensively targeted by SWIFT + UVOT, from the UV domain to the blue optical bands. Unfortunately, the optical and NIR ground-based coverage is not ideal, suffering from some observational gaps. However, additional contributions of unfiltered photometry from amateur astronomers and R-band photometry obtained with MASTER facilities allowed us to to improve the light curve sampling at least in the R band. Additional multi-band pho-

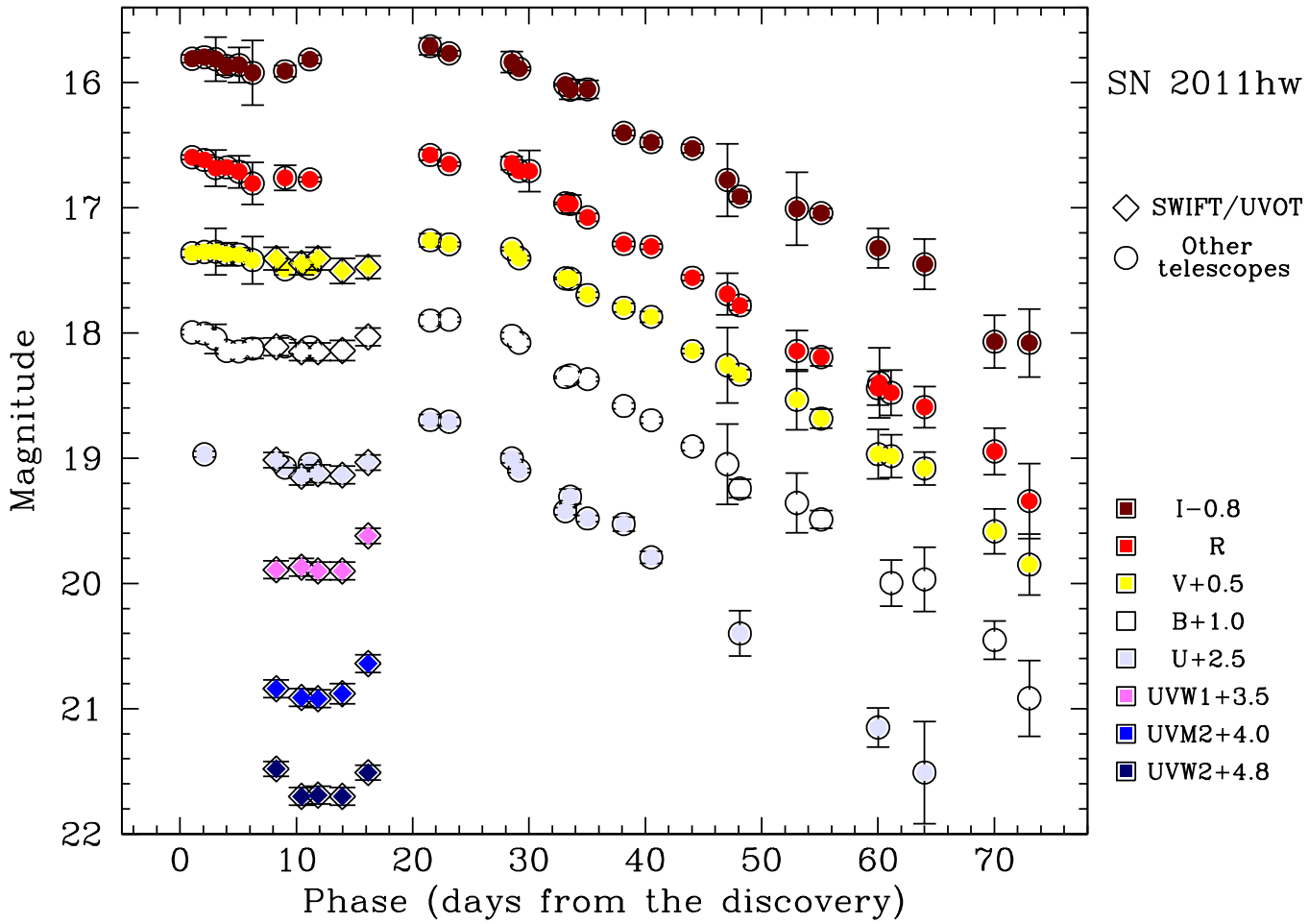

Figure 3. UV and optical light curves of SN 2011hw. Swift/UVOT optical-band magnitudes have been shifted by +0.054 mag in U and −0.025 mag in V to match the ground-based measurements.

tometry measurements as derived from the accurately calibrated XShooter spectra [9] were also used (see Table A3). The resulting light curves of SN 2010al are shown in Figure 2. The left panel of Figure 2 shows the early UV-to-NIR evolution (up to ∼2 months), whilst the right panel includes also the late-time optical+NIR observations obtained when the SN was recovered after the seasonal observational gap. At late times the object was detected only once in the NIR bands, while it was not detectable in optical observations, and we could only estimate upper detection limits. We note that the decline rate in the NIR bands after the seasonal gap is marginally flatter than the decline rate expected when the ^{56}Co decay to ^{56}Fe powers the SN light curve (assuming full gamma-ray trapping). Unfortunately, no information on the decline rate can be inferred from the late-time optical observations.

[9] R-band VLT acquisition images were used to properly scale in flux the XShooter spectra, and spectro-photometric measurements were performed using the package *STSDAS* in IRAF. A final uncertainty of 10 per cent in the flux calibration has been adopted for the XShooter spectra (Section 4).

The photometric follow-up campaign of SN 2011hw in the optical bands lasted about 2.5 months, after which the object disappeared behind the sun. Additional late-time imaging was obtained about 6-7 months later, but the object was below the detection threshold. In fact, no source was detected at the SN position in TNG+Dolores images obtained on July 25th, 2012 (to limiting magnitudes R = 23.2 and I = 23.1) and in very deep WHT+ACAM images obtained on August 21st, 2012 (to limiting magnitudes U = 23.3, B = 23.9, V = 24.2). The light curve (see Figure 3) is peculiar, showing a modest decline in all bands soon after the discovery lasting about 1 week. This was followed by a re-brightening leading to a second maximum at phase of about 3 weeks. This was already noted by Smith et al. (2012), and interpreted as an additional luminosity input from interaction when the shock reaches a higher density CSM shell. Similar re-brightenings in the light curves have been onserved also in the transitional Type Ibn/IIn SN 2005la (Pastorello et al. 2008b) and the Type Ibn iPTF13beo (Gorbikov et al. 2014).

The secondary maximum is then followed by a fast linear decline, which is steeper in the blue bands, with slopes:

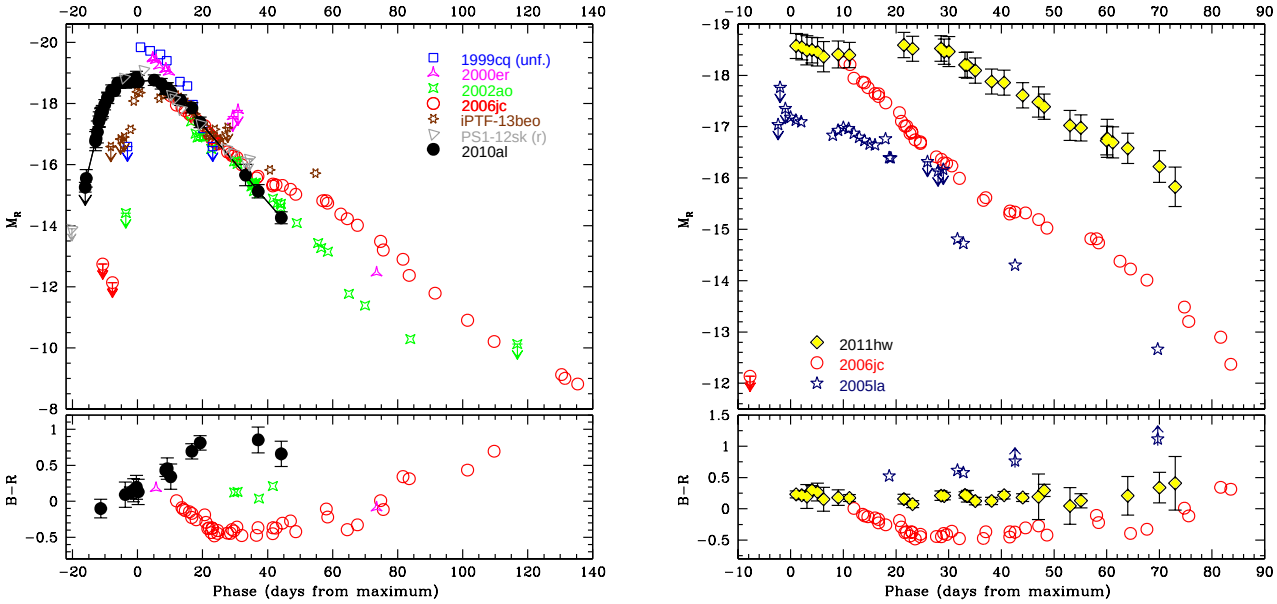

Figure 4. Top-left: R-band absolute light curves of SN 2010al and other Type Ibn SNe, including SNe 1999cq, 2000er, 2002ao, 2006jc, PS1-12sk and iPTF-13beo (Matheson et al. 2000; Pastorello et al. 2007, 2008a; Foley et al. 2007; Sanders et al. 2013; Gorbikov et al. 2014). SN 2010al is marginally fainter at peak than other SNe Ibn shown here, and has a slower rise to maximum. **Bottom-left:** $B-R$ colour curves for the same sample of SNe Ibn. **Top-right:** R-band absolute light curves of the Type Ibn/IIn SNe 2011hw and 2005la, compared with the prototypical SN Ibn 2006jc. For SNe 2011hw and 2005la, we adopt the discovery epochs as reference dates for the maximum. For SN 2005la, only the most significant detection limits are shown. **Bottom-right:** $B-R$ colour curves for SNe 2011hw, 2005la and 2006jc. Data have been corrected for interstellar reddening.

$\Delta U = 6.8 \pm 0.2$ mag/100^d; $\Delta B = 5.8 \pm 0.2$ mag/100^d; $\Delta V = 5.2 \pm 0.2$ mag/100^d; $\Delta R = 5.5 \pm 0.1$ mag/100^d; $\Delta I = 4.7 \pm 0.2$ mag/100^d. Additional early-time UV photometry was obtained with SWIFT/UVOT showing the same re-brightening to the secondary maximum as the optical bands. Unfortunately, the SWIFT campaign was suspended after 8 days, and no UV observations were obtained during the second peak.

In Figure 4 (top-left panel) the absolute R-band light curve of SN 2010al is shown along with those of the Type Ibn SNe 1999cq (Matheson et al. 2000), 2006jc (Pastorello et al. 2007, 2008a; Foley et al. 2007), PS1-12sk (Sanders et al. 2013), iPTF-13beo (Gorbikov et al. 2014), 2000er and 2002ao (Pastorello et al. 2008a). SN 2010al (peaking at an absolute magnitude $M_R = -18.86 \pm 0.21$ on $JD = 2455284.3 \pm 1.1$) is slightly less luminous than both SN 2000er and SN 1999cq, and has a symmetric light curve peak, with a slow rise but a similar post-peak decline rate. In the top-right panel of Figure 4, the light curve of SN 2011hw is compared with those of SN 2006jc and the Type Ibn/IIn SN 2005la (Pastorello et al. 2008b). SN 2011hw has an absolute magnitude at the second maximum of $M_R = -18.59 \pm 0.25$, which is very close to the magnitude at discovery. Although the luminosity of SN 2005la is lower and its light curve has some scatter, the indication is that SN 2005la, like SN 2011hw, has a non-monotonic behaviour after the first maximum, possibly related to an enhanced contribution of the ejecta interaction with a higher-density CSM. A shoulder is also visible in the optical light curve of SN 2006jc after $\sim$ 40 days, but it was shown to be related to the formation of dust in a post-shock cool dense shell (see e.g. Smith et al. 2008; Mattila et al. 2008). One of the effects of dust formation is the attenuation of the light at optical wavelengths and the enhanced emission in the infrared domain. The lack of NIR observations does not allow us to verify whether dust has formed in the ejecta of SN 2011hw or in the circumstellar environment.

In the bottom panels of Figure 4 the extinction-corrected $B-R$ colour curves of our Type Ibn SN sample are shown. The comparisons show that there is some heterogeneity in the colour evolution of SNe Ibn. In comparison with the other objects, SN 2010al shows an opposite colour trend (bottom-left panel), reaching a $B-R$ colour maximum of $\sim$1 mag at about 30 days past maximum, while at the same phase the colour of SN 2006jc was extremely blue ($B-R \approx -0.5$ mag). After $\sim$40 days from maximum, SN 2006jc and the transitional SNe 2011hw and 2005la show a moderate trend toward redder colours (bottom-right panel), which may be a signature of dust formation. However, we agree with the findings of Smith et al. (2012) that the available spectra of SN 2011hw do not show a clear evidence for blue-shifted spectral line peaks, and this would argue against the dust formation in this object.

3.4 Quasi-bolometric light curves

Quasi-bolometric light curves for SNe 2010al and 2011hw have been computed either by integrating the fluxes in the optical bands only, and - in the case of SN 2010al - including also the UV and NIR contributions to the to-

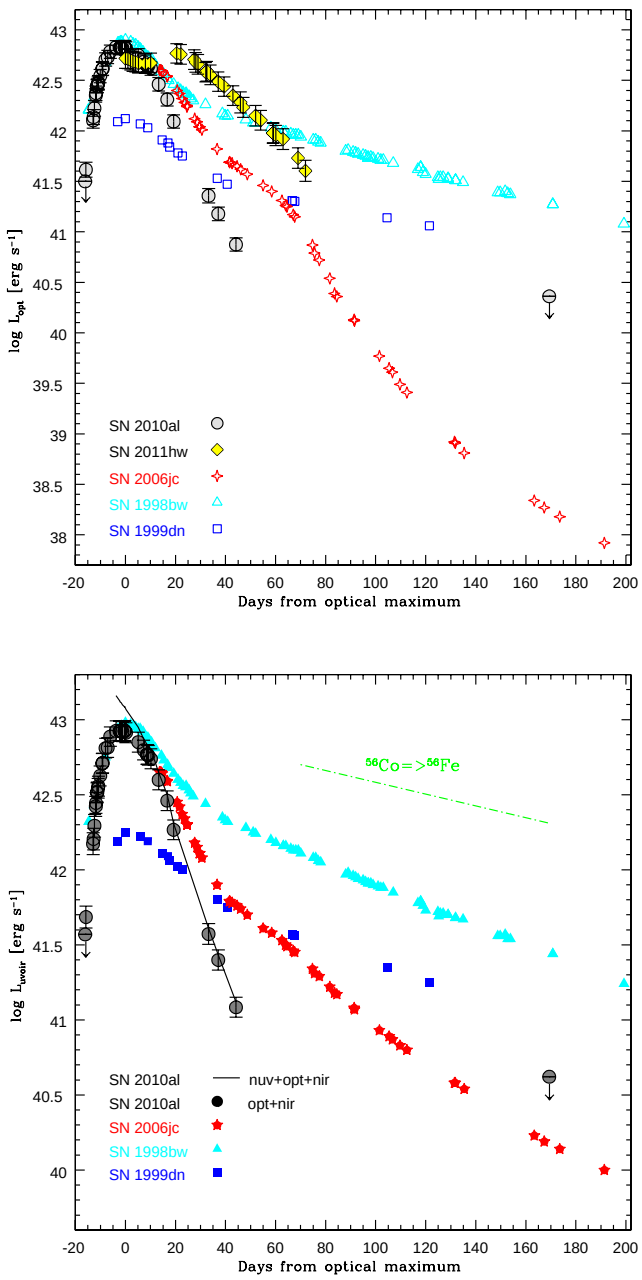

Figure 5. Quasi-bolometric light curves of the Type Ibn SNe 2006jc, 2011hw and 2010al compared with those of the normal SN Ib 1999dn (Benetti et al. 2011) and the broad-lined Ic SN 1998bw (Patat et al. 2001, and references therein). **Top:** Pseudo-bolometric light curves for the SN sample have been computed by integrating the fluxes in the optical bands only. **Bottom:** The pseudo-bolometric light curves have been obtained by integrating the broadband fluxes in the optical and NIR domains. In the case of SN 2010al, also an *uvoir* curve obtained including the near-UV contribution is shown (solid line), although limited to phases later than -3.7 days from maximum. Error-bars have been reported for SNe 2010al and 2011hw, and account for uncertainties in the distance and the reddening estimates, spectral energy distribution fitting and photometric errors.

tal flux. Occasionally, photometric data in a given filter were not available. The flux contribution of the missing band was then obtained by interpolating the fluxes between epochs when photometric observations were available or, when necessary, by extrapolating the missing photometry from the earliest/latest available epoch, assuming a constant colour evolution. The flux in individual bands was corrected for the adopted extinction and used to derive the spectral energy distribution that was then integrated to derive the quasi-bolometric flux. The total flux was finally converted in luminosity using the extinction values and the distance moduli discussed in Section 3.2. The resulting quasi-bolometric light curves are shown in Figure 5, along with those of the prototypical SN Ibn 2006jc (Foley et al. 2007; Pastorello et al. 2007, 2008a; Mattila et al. 2008), the normal SN Ib 1999dn (Benetti et al. 2011) and the broad-line SN Ic 1998bw (Galama et al. 1998; McKenzie & Schaefer 1999; Patat et al. 2001; Sollerman et al. 2002). The top panel of Figure 5 shows the "optical" pseudo-bolometric light curves, the bottom panel reports the pseudo-bolometric light curves obtained by including also the flux contribution in the NIR domain. For SN 2010al, the UV to NIR (*uvoir*) curve is also shown, plotted with a solid line. We note that we can provide only a lower limit ($L > 5.5 \times 10^{42}$ erg s^{-1}) for the maximum luminosity of SN 2011hw, since the object was probably discovered after maximum, and NIR observations were not available.

The quasi-bolometric light curve of SN 2010al peaks at a maximum luminosity of about 10^{43} erg s^{-1}, which is similar to the peak luminosity of SN 1998bw. We also note that NIR contribution is small around maximum, but increases with time becoming significantly larger at post-peak phases. A similar behaviour was also observed in SN 2006jc, although in that case the late NIR contribution was much more significant. A strong deficit in the optical light curve was observed at >40 days past maximum (Smith et al. 2008; Mattila et al. 2008, see also Figure 5) and was balanced by a clear NIR excess. The resulting quasi-bolometric light curve of SN 2006jc showed a decline that was consistent with a ^{56}Co-powered event assuming a complete γ-ray trapping (Figure 5, bottom). We remark that in SN 2010al there is a single late-time detection of the SN in the NIR bands and no detection in the optical bands at nebular phases. So, the luminosity estimate at ∼162 days in Figure 5 has to be regarded as an upper limit and, hence, we cannot provide a reliable estimate for the ^{56}Ni mass.

4 SPECTROSCOPY

Both SN 2010al and SN 2011hw have extensive spectroscopic sequences, and the reduction of the spectra was performed using standard *IRAF* tasks. The preliminary reduction steps included overscan and bias corrections, flat-fielding and trimming, following the same prescriptions as imaging data. For the NIR spectra, the contribution of the night sky background was removed by subtracting from each other two consecutive exposures taken with the source in different positions along the slit. The spectra were then optimally extracted to remove all background contamination and hot pixels. Then, spectra of the science targets were wavelength calibrated using arc lamp comparison spectra,

Table 1. Log of spectroscopic observations of SNe 2010al and 2011hw.

SN 2010al						
Data	JD+ 2455000	Phase (days) after core-collapse	Phase (days) after discovery	Instrumental configuration	Range (Å)	Resolution* (Å)
20Mar10	275.65	7.7	7.1	DuPont + B&C	3700-9250	7
25Mar10	280.55	12.6	12.0	VLT-UT2 + XShooter	3000-24800	0.8;0.8;3.2
29Mar10	284.50	16.5	16.0	VLT-UT2 + XShooter	3000-24800	0.8;0.8;3.2
30Mar10	286.38	18.4	17.9	WHT + ISIS	3000-10000	4.9;9.5
01Apr10	288.47	20.5	19.9	NOT + ALFOSC	3200-9000	18
06Apr10‡	293.42	25.4	24.9	Ekar182 + AFOSC	4100-8100	24
07Apr10	294.49	26.5	26.0	VLT-UT2 + XShooter	3000-24800	0.8;0.8;3.2
18Apr10	304.58	36.6	36.1	NTT + EFOSC2	3650-9050	27
19Apr10	305.56	37.6	37.0	NTT + SOFI	9350-16450	25
22Apr10	309.42	41.4	40.9	TNG + NICS	8700-14550	19
24Apr10	311.47	43.5	42.9	TNG + LRS	3200-7950	15
29Apr10	316.44	48.4	47.9	TNG + LRS	5050-9350	14
05May10	322.42	54.4	53.9	TNG + LRS	5000-10200	9.5
11May10	328.48	60.5	60.0	VLT-UT2 + XShooter	3000-24800	0.8;0.8;3.2
SN 2011hw						
Data	JD+ 2455000	Phase (days) after core-collapse	Phase (days) after discovery	Instrumental configuration	Range (Å)	Resolution* (Å)
19Nov11	885.26	15.3	1.0	Ekar182 + AFOSC	3550-8200	12;24
20Nov11	886.30	16.3	2.1	Ekar182 + AFOSC	3500-8150	24
24Nov11	890.43	20.4	6.2	Ekar182 + AFOSC	3600-8200	24
27Nov11	893.32	23.3	9.1	Ekar182 + AFOSC	3600-8200	12
28Nov11	894.40	24.4	10.2	NOT + ALFOSC	3300-9100	14
29Nov11	895.43	25.4	11.2	CAHA2.2 + CAFOS	5800-9600	6
17Dec11	913.34	43.3	29.1	TNG + LRS	3250-10350	15;14
18Dec11‡	914.29	44.3	30.1	Ekar182 + AFOSC	3500-8200	24
21Dec11	917.31	47.3	33.1	WHT + ISIS	3100-10400	5;9
01Jan12	928.31	58.3	44.1	CAHA2.2+CAFOS	3350-8850	14
17Jan12	944.36	74.4	60.1	TNG + LRS	3300-8050	15
18Jan12	945.36	75.4	61.1	TNG + LRS	5050-9650	14
29Jan12	956.36	86.4	72.1	NOT + ALFOSC	3400-9100	18

* As measured from the FWHM of the night sky lines. ‡ Poorer signal-to-noise spectra, not shown in Figures 6 and 8.

and were finally flux-calibrated using sensitivity curves obtained from spectro-photometric standard star spectra.

The higher resolution XShooter spectra were processed using of the dedicated ESO pipeline[10]. For each of the UV, optical and NIR channels, linearized, sky-subtracted and wavelength-calibrated 2-dimensional spectra were obtained from the curved Echelle orders of XShooter. The 1-dimensional spectra were obtained through the optimal extraction as for the low-resolution spectra. Relative flux calibrations were performed through spectro-photometric standards for which flux tables extending from the UV to the NIR domains are available. The flux tables were taken from the dedicated ESO web site.[11]

For all spectra, the accuracy of the spectroscopic flux calibration was checked using the available SN photometry. In case of discrepancy, the spectral fluxes were rescaled to match the photometric data. The expected uncertainty in the flux calibration is about 10 per cent. Finally, spectra of telluric standards were used to remove the broad atmospheric absorption bands from the SN spectra.

The log containing the spectroscopic observations of the two events is provided in Table 1.

4.1 Spectral sequence of SN 2010al

SN 2010al was observed in optical and NIR spectroscopy from day 7 after the discovery to about day 60. In Figure 6 the sequence of our good signal-to-noise spectra of SN 2010al is shown, with the optical spectra being in the top panel, and the NIR spectra in the bottom panel.

Our earliest spectrum shown in Figure 6 is the classification spectrum of Stritzinger et al. (2010). The spectrum is peculiar, showing a blue continuum and relatively prominent Balmer lines in emission. Hα has a narrow unresolved component (< 360 km s^{-1}) possibly due to interstellar gas contamination, superposed on an intermediate component with a full width at half maximum (FWHM) velocity $v_{FWHM} \approx 1800$ km s^{-1}.

The most prominent emission feature lies in the blue region of the spectrum (at about 4660 Å) and shows a double-

[10] *http://www.eso.org/sci/software/pipelines/*
[11] *https://www.eso.org/sci/observing/tools/standards/spectra.html*

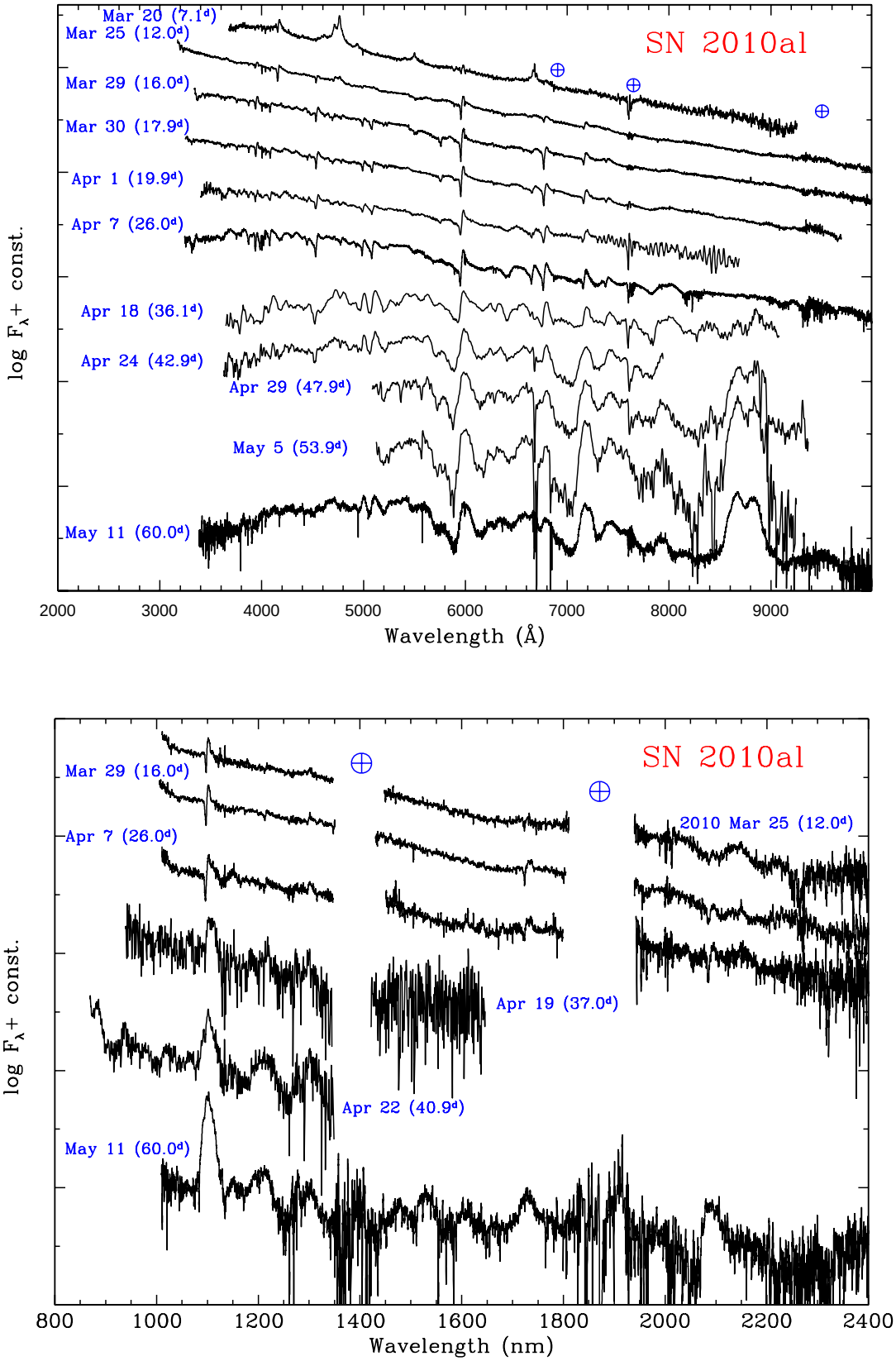

Figure 6. Optical (**top panel**) and NIR (**bottom panel**) spectra of SN 2010al. No redshift or reddening corrections have been applied. The positions of the most important telluric bands are marked with "⊕". The phases reported in brackets are days after discovery.

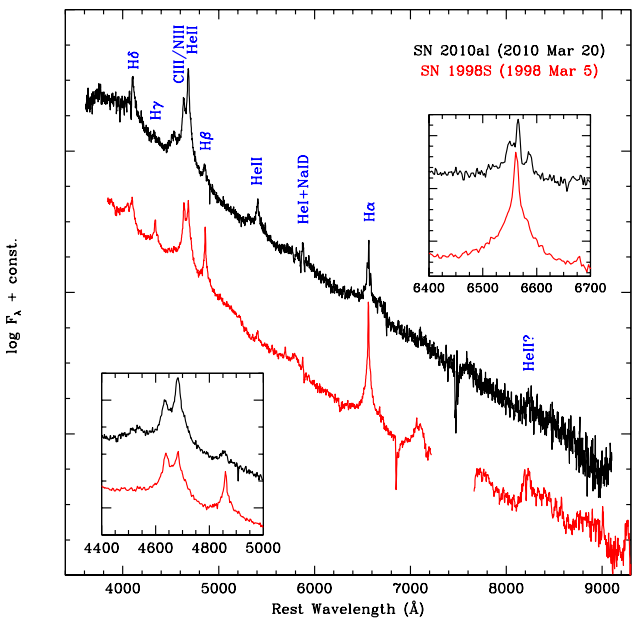

Figure 7. Comparison between the earliest optical spectra of SN 2010al and the Type IIn SN 1998S (Fassia et al. 2001). The two spectra are reddening- and redshift-corrected. The inserts shows a blow up of the region between 4400 and 5000 Å (bottom-left) and the region of Hα (top-right) in the two spectra.

peaked profile. The redder component peaks at 4684 Å and is very likely He II λ4686, while the bluer emission peaks at 4646 Å, and is probably a blend of C III λ4648 and N III λ4640. We note that these lines, identified also by Cooke et al. (2010) and Silverman et al. (2010), are often observed in Wolf-Rayet winds. A very similar feature was also observed in very early spectra of the Type IIn SNe 1998S (Fassia et al. 2001), 2008fq (Taddia et al. 2013), and also in the classification spectrum of LSQ13fn (Sollerman et al. 2013). A comparison with the spectrum of SN 1998S at 3.3 days after the discovery presented by Fassia et al. (2001) is shown in Figure 7; the two inserts emphasize the regions of the peculiar spectral feature at $\sim$ 4600-4700 Å and that of Hα. The identification of He II in both SNe is safe, since He II λ5411 is also detected, with $v_{FWHM} \approx 2250$ km s^{-1}. Another, weaker feature is detectable at about 4460-4560 Å and is probably a line blend of various ionized elements, including He II λ4541, although we cannot exclude a minor contribution from the He I λ4471 line (see the insert in Figure 7). We also tentatively identify He II λ8236, following Fassia et al. (2001).

The second spectrum of SN 2010al (day 12 after the discovery) is very different, and this suggests us to revise the classification of this object as a Type Ibn SN (see Section 1). The spectrum is still dominated by a blue continuum ($T_{bb} = 12800 \pm 400$ K), but now the most remarkable lines visible in the spectrum are He I, with unusually narrow P-Cygni profiles. The position of the minimum of the blue-shifted absorption component suggests velocities of the He-rich material of about 1000-1100 km s^{-1}. The feature detected in the first spectrum at about 4600-4700 Å is now much weaker, although it still shows a double-peaked profile. A very weak hump probably due to Hα is also detected. Very narrow absorptions of Ca II H&K and Na ID are attributed to material lying along the line of sight and are unrelated to the SN environment.

In the third spectrum (day 16, $T_{bb} = 11900 \pm 400$ K), He I P-Cygni lines with a measured expansion velocity $v \approx$ 1050-1150 km s^{-1} become more and more prominent. We note that these P-Cygni He I lines are likely produced in He-rich CSM moving at a velocity of above 1000 km s^{-1} which was initially ionized (e.g. at the epoch of our first spectrum), and is now recombining. At this phase, together with the He I lines, probably other features (including weak Fe II lines) are detected. The Wolf-Rayet feature at about 4600-4700 Å has completely disappeared, while Hα is still barely detected (with expansion velocity of about 1100 km s^{-1}). The following spectra (phases 18 and 20 days after discovery) do not show a significant evolution.

The XShooter spectrum at day 26 has a redder continuum ($T_{bb} = 9100 \pm 500$ K), and many new P-Cygni SN lines are now detected, including Ca II H&K and Fe II. A few weak lines of He I are now visible in the NIR region. In particular, the He I λ20581 line is clearly detected. In addition, Hα is visible with a P-Cygni profile, and with an expansion velocity that is comparable with that of the He I, Ca II and Fe II lines, i.e. around 1300-1400 km s^{-1}.

The spectrum obtained 36 days after discovery shows major changes. The continuum is now much redder and (especially at red wavelengths) the emission components start to dominate over the absorptions. In addition the lines are broader (1900-2300 km s^{-1}). Hα is not visible anymore, and the NIR Ca II triplet is now clearly detected. A broad line likely due to a blend including also O I $\lambda\lambda$7772-7775 is one of the most prominent spectral features. The two NIR spectra at days 37 and 41, despite the low signal-to-noise, show that the most prominent line in the NIR region is He I λ10830, almost purely in emission, with a FWHM velocity of about 5000 km s^{-1}.

The following spectra (days 43, 48 and 54) show a strong pseudo-continuum below 5600 Å (which is much stronger in SN 2011hw, see below), in analogy with that observed in other SN 2006jc-like events (but also in Type IIn SNe). The lines have a similar width as in the previous NIR spectra (4000-5000 km s^{-1}), and the most prominent feature is now the broad NIR Ca II triplet in emission, with a double-peaked profile and a total FWHM of about 12000 km s^{-1}. The last XShooter spectrum (day 60) confirms most characteristics of the previous spectra, with a significant blue pseudo-continuum where He I and Fe II absorptions are still well visible. The lines of He I λ5876 (possibly blended with Na ID), λ7065 and λ10830 are now prominent in emission although a residual broad P-Cygni absorption is still barely visible. Other He I lines are detected in the NIR, in particular λ15084, λ17002, $\lambda\lambda$18685-18697 and λ20581. The FWHM velocity of all these lines from a Gaussian fit is about 5000 $\pm$ 1000 km s^{-1}. The apparent broadening of the spectral lines with time indicates that the photosphere recedes with time from the shocked CSM to the SN ejecta. This explanation is supported by the Gaussian emission lines that do not show evident boxy profiles. Other features that can be observed in the day 60 spectrum are a very prominent Ca II NIR triplet in emission (blended with O I λ8448) and Mg I λ7659. Mg lines can also contribute to shaping the ap-

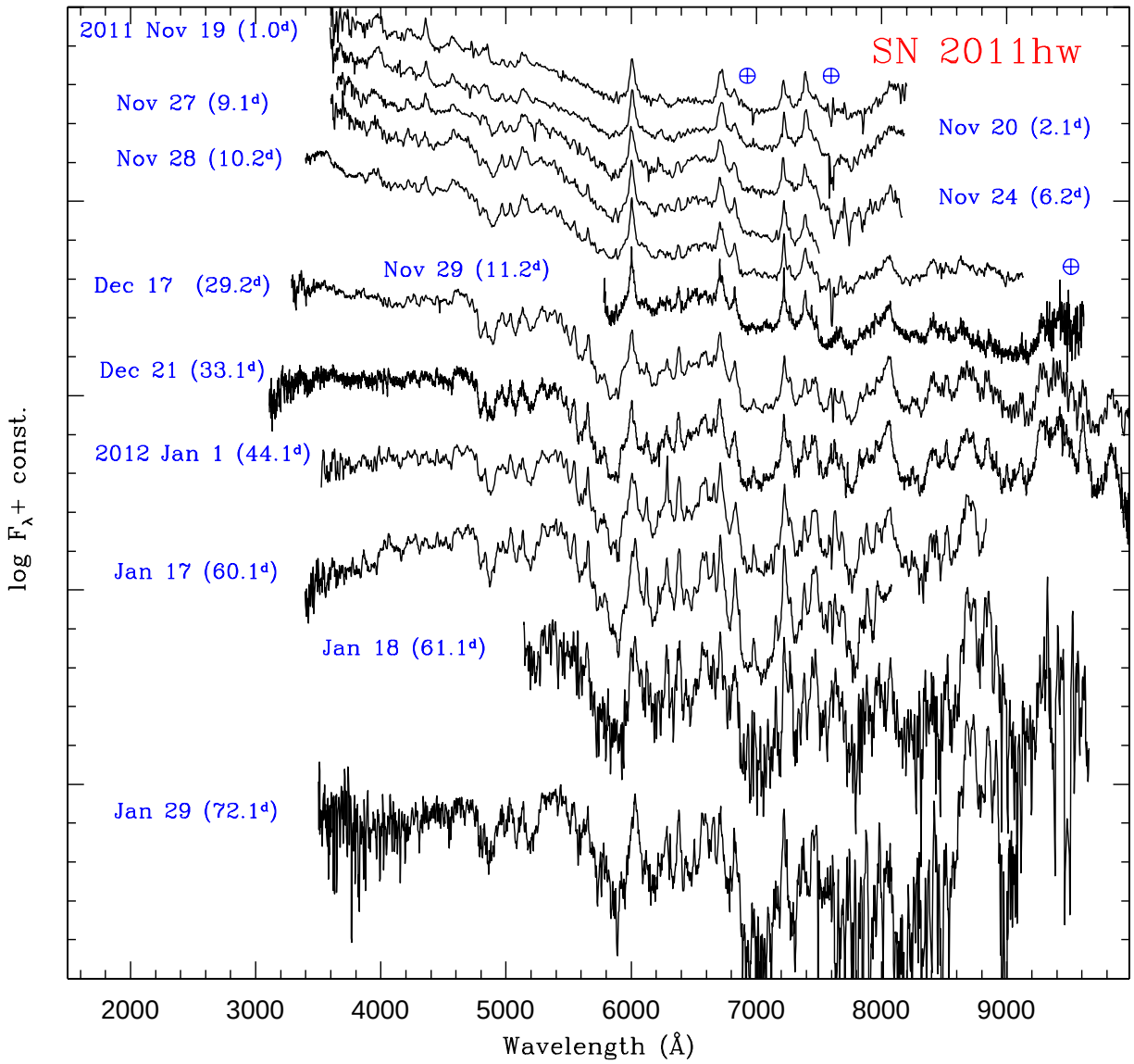

Figure 8. Optical spectral sequence for SN 2011hw. No redshift or reddening corrections have been applied. The positions of the most important telluric bands are marked with "⊕". The phases reported in brackets are days after discovery.

parent emission bumps at ∼ 4600 Å, 5200 Å and 9000-9500 Å (blended with O I). The broad bump around 6600 Å can be due to a blend of different lines, including C II, as proposed by Sanders et al. (2013). Finally, a strong emission feature is detected at ∼ 7300 Å, that is identified as [Ca II] $\lambda\lambda$7291-7324 (possibly blended with C II λ7234 and He I λ7281, see Sanders et al. 2013), growing in intensity.

4.2 Spectral sequence of SN 2011hw

SN 2011hw was extensively monitored in optical spectroscopy. The follow-up campaign started soon after the SN discovery, and lasted about 70 days. The collection of spectra is displayed in Figure 8. The spectra show a modest evolution during the entire observational period, confirming the late discovery of SN 2011hw. The strongest features are the He I lines, showing complex profiles with broader and narrower components (see below). A double-component Hα is also detected, though quite weak. Other Balmer lines, usually prominent in Type IIn SNe, are weak in SN 2011hw. The spectrum is dominated by a pseudo-continuum bluewards of ∼5600 Å, and relatively narrow emission features more prominent in the red spectral region. The nature of the blue pseudo-continuum was widely discussed by Turatto et al. (1993), Smith et al. (2012) and Stritzinger et al. (2012), who suggested that it is the result of the blending of a forest of narrow and intermediate-width Fe lines, as in the case of SN 2006jc ($v_{FWHM} \approx$ 2000-2500 km s^{-1}, Smith et al. 2008; Chugai 2009) or SN 2005ip ($v_{FWHM} \approx$ 150-200 km s^{-1}, Smith et al. 2009;

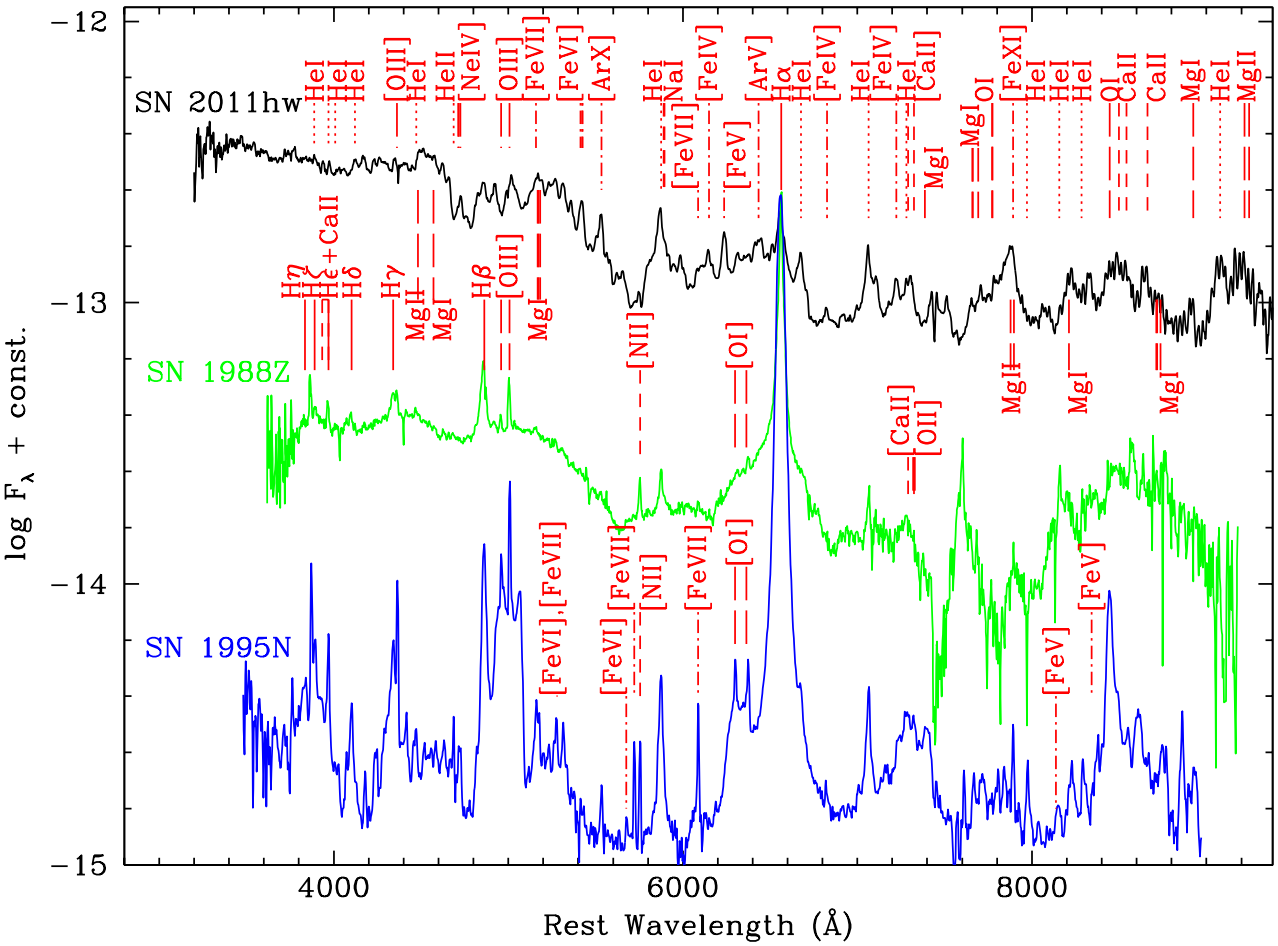

Figure 9. The 2011 December 17 spectrum of SN 2011hw is shown together with spectra of the Type IIn SNe 1988Z and 1995N. The most important lines detectable in the spectra are marked.

Stritzinger et al. 2012). These lines might explain at the same time the apparent step in the continuum at ∼5600 Å, the broad "W"-shape feature at 4600-5200 Å (but also some He I lines may contribute), and the broad bump between 6100 Å and 6600 Å. Smith et al. (2012) noted a major property that distinguishes SN 2011hw spectra from those of SN 2006jc: the presence of narrow, high-ionization circumstellar lines. A comprehensive line identification is shown in Figure 9, where a spectrum of SN 2011hw (December 17, 2011) is shown along with those of two interacting, H-rich SNe, viz. the Type IIn SNe 1995N (Pastorello et al. 2005) and 1988Z (Turatto et al. 1993). We used the line identification performed by Fransson et al. (2002) and Turatto et al. (1993) as guides for the identification of the metal lines in our SN 2011hw spectrum. We confirm the detection of many high-ionization lines of Smith et al. (2012), including [Ne IV] λ4714, λ4716, λ4726, [Ar X] λ5536, [Ar V] λ6435 and a number of [Fe IV], [Fe V] [Fe VI] and [Fe VII] lines. Other coronal lines clearly detected in SN 2005ip are weak or absent in SN 2011hw (Smith et al. 2012). A weak, narrow [N II] λ5765 feature is also visible. The line doublet of [O III] $\lambda\lambda$4959,5007, occasionally identified in spectra of interacting SNe, is possibly seen also in SN 2011hw, whilst the detection of [O I] and [O II] lines (which are common in Type IIn SNe, though with different strengths, being prominent in SN 1995N and weaker in SN 1988Z) is not unequivocal.

Smith et al. (2012) attributed the presence of coronal lines to high-energy photons produced in shocked material that were able to penetrate the CSM up to the external unshocked regions. The higher resolution spectra presented by Smith et al. (2012, see their Figure 5) provide evidence for the presence of narrow He I components on top of broader wings. In our highest resolution spectrum of November 29 obtained with CAFOS, the narrow lines are visible but not fully resolved. We measure a FWHM velocity of <220 km s^{-1} for both He I lines and Hα, while the intermediate components extend to about 2000 km s^{-1}. Our measurements are in excellent agreement with those of Smith et al. (2012). Intermediate components of Mg I (e.g. λ4571, $\lambda\lambda$5167-5184, λ7659, λ8213, λ8924, λ9256 and $\lambda\lambda$9415-9438), Mg II (λ4481, $\lambda\lambda$7877-7896 and $\lambda\lambda$9218-9244), O I (λ7774, λ8222, λ8446, $\lambda\lambda$9261-9266) and Ca II in the NIR region are clearly detected. Some of these lines possibly show narrow components.

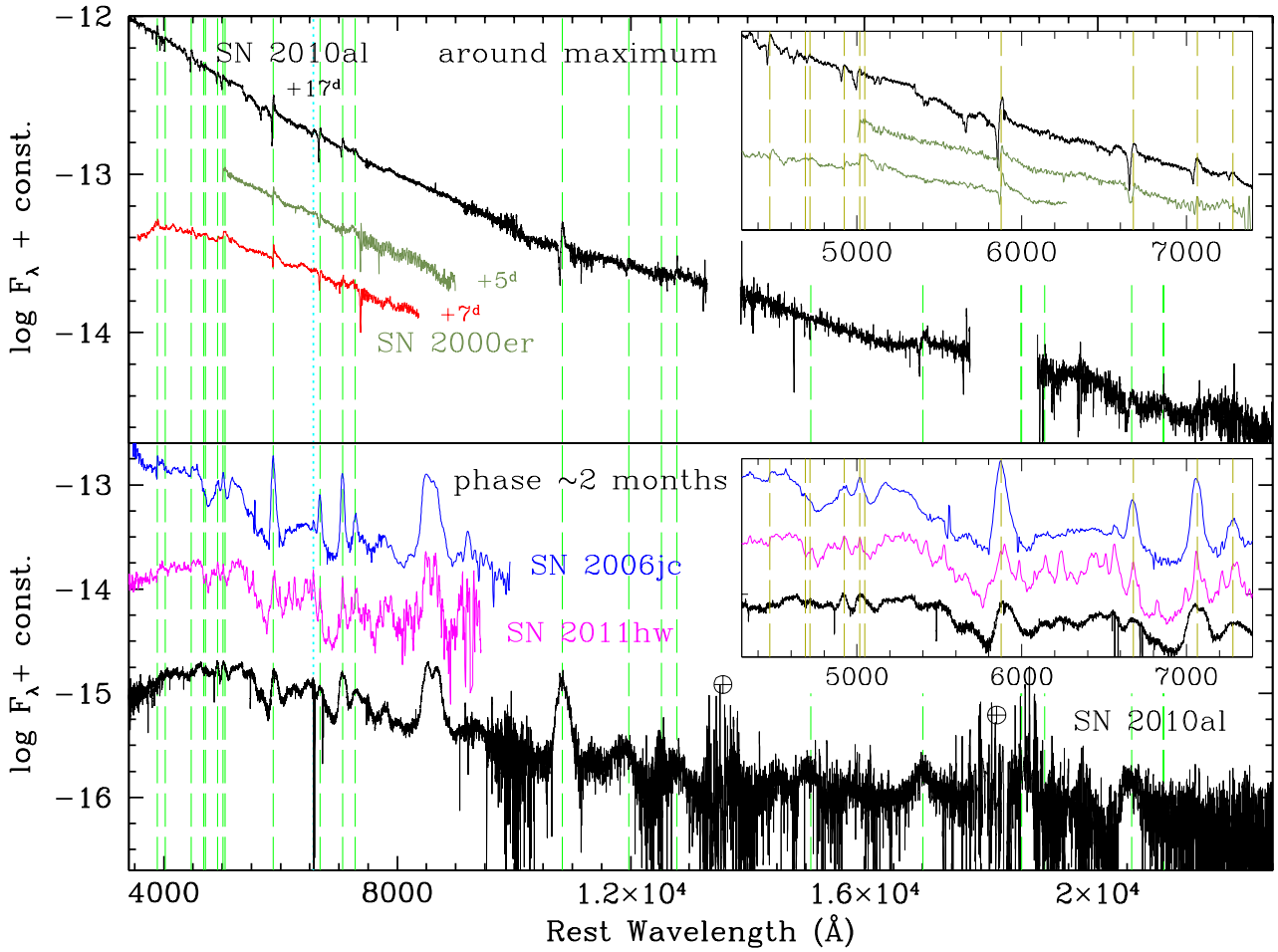

Figure 10. Comparison of early-time (**top**) and ∼ 2-months-old (**bottom**) spectra of SN 2010al with those of other Type Ibn SNe at similar phases. The phases labelled in the upper panel are from the epoch of the core-collapse. The rest frame positions of the strongest He I lines are marked with green dashed vertical lines. The cyan short-dashed line marks the position of Hα. The inserts show the regions where the most prominent He I features visible in the spectra are located, viz. between 4300 Å and 7400 Å.

The intermediate components probably arise from shocked material, while the narrow components are linked to the unshocked CSM (Smith et al. 2012). Consequently, the width of the narrow components gives some clues on the velocity of the pre-SN stellar wind. In SN 2011hw, the narrowest spectral lines have $v_{FWHM} \sim 200$ km s^{-1}, which is about one order of magnitude lower than the lowest velocity component measured in SN 2006jc. The former value is unusually low for a typical Wolf-Rayet wind, such as that observed in the CSM of SN 2006jc (Pastorello et al. 2007; Foley et al. 2007; Smith et al. 2008). This, in combination with the clear detection of H in the spectra, supports one of the main conclusions of Smith et al. (2012), that the progenitor of SN 2011hw was not a proper Wolf-Rayet star, but probably a transitional object that retained some LBV properties.

4.3 Comparison of Type Ibn SN spectra

In Figure 10 (top)[12] an early-time spectrum of SN 2010al is compared with early optical spectra of the Type Ibn SN 2000er (Pastorello et al. 2008a). The early spectroscopic similarity of the two objects is evident. The most important He I lines are marked with vertical dashed green lines, the strongest being λ4471, λ5876, λ6678, λ7065, λ10830 (the most prominent He I feature), λ17002, $\lambda\lambda$18685-18697 (though contaminated by a wide telluric absorption band) and λ20581. Hα, with a P-Cygni profile, is barely detected in these early spectra. In Figure 10 (bottom) a late spectrum of SN 2010al is compared with spectra of SN 2011hw and 2006jc (Pastorello et al. 2007) at similar phases. The spectra of the three objects share a very similar blue pseudo-continuum and the most prominent broader spectral lines. However, there are some subtle differences. In particular,

[12] A similar figure was shown in Pastorello et al. (2012), but without the SN 2011hw spectrum shown here in the bottom panel.

Hα is still visible as a pure emission -though quite weak- in SN 2011hw, while it is not unequivocally detected in the late-time spectra of SNe 2006jc and 2010al.

Although there is some heterogeneity in Type Ibn SNe, in general these objects show similar spectral properties and evolution, both in terms of the overall shape of the pseudo-continuum and in the line identification, profiles and velocities, suggesting that the physical conditions in the line-forming gas regions are not significantly different among the SNe of our sample. All of this would indicate a rather similar composition and final configuration in the progenitors of Type Ibn SNe.

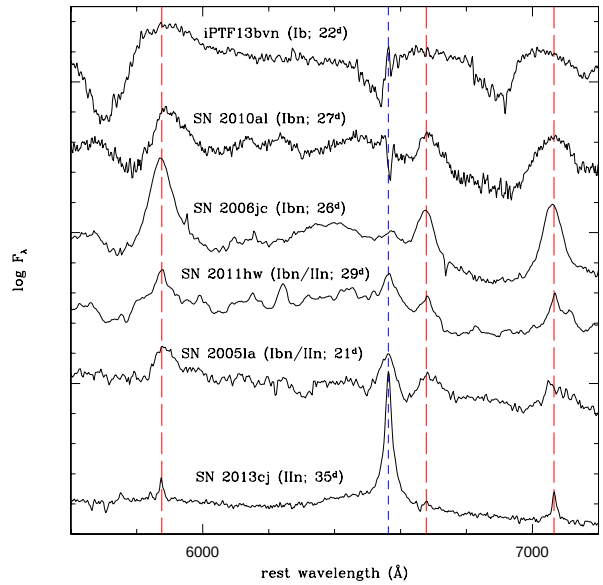

Figure 11. Comparison of a sample of SN spectra obtained a few weeks after their maximum. The phases from maximum are reported in brackets. The sample includes: the Type Ib SN iPTF13btv (Srivastav et al. 2014), the Type Ibn SNe 2010al and 2006jc, the Type Ibn/IIn SNe 2011hw and 2005la and the Type IIn SN 2013cj (from the Padova-Asiago SN Archive). Dashed red lines mark the position of strong He I features, the short-dashed blue line marks the position of Hα.

5 DISCUSSION AND SUMMARY

Type Ibn SNe represent a small sub-group of CC SNe whose ejecta appear to interact with a dense He-rich, H-poor circumstellar shell. From this point of view, the relative H-to-He abundance in the CSM and the different velocities inferred from the narrow lines (usually $<10^3$ km s^{-1} in SNe IIn, 2-4$\times10^3$ km s^{-1} in SNe Ibn) help to discriminate the observed properties of SNe Ibn from those of classical SNe IIn (see e.g. Taddia et al. 2013). However, SN 2011hw and, even more, SN 2005la (Pastorello et al. 2008b) are quite peculiar in our sample. They show a non-monotonic post-maximum light curve decline and clear signatures of narrow Balmer lines in their spectra, suggesting that they are transitional objects between the two CC SN sub-types. Another object, iPTF13beo, has a double peak in the light curve (Gorbikov et al. 2014), but it does not show H lines in the spectra.[13] The observational evidence links SNe Ibn to Wolf-Rayet stars, and SNe IIn (or, at least, some of them) to LBVs (e.g. Kotak & Vink 2006; Smith & Owocki 2006; Gal-Yam et al. 2007; Trundle et al. 2008, 2009; Kiewe et al. 2012; Groh et al. 2013a,b). In this context, both SN 2011hw and SN 2005la can be considered as the result of the explosion of massive stars that were transiting from the LBV to the WR stages (Pastorello et al. 2008b; Smith et al. 2012).[14] Smith et al. (2012) provided robust evidences of the link of SN 2011hw to early WN stars with some residual H, or even Opfe/WN9 stars (although the wind velocity observed in the latter is significantly lower than that observed in the CSM of SN 2011hw). In this case, if the progenitor star belongs to a massive binary system, the mass transfer from the companion might enable the LBV to WN or Opfe/WN9 transition. As an intriguing consequence, SNe Ibn might be regarded as transitional objects in a sort of sequence between WR-related events (some Type Ib/c SNe) and LBV-related events (some SNe IIn). The existence of a continuity from SNe IIn to stripped-envelope SNe is illustrated in the comparison among post-maximum spectra in Figure 11. Although we admit that this conclusion is speculative, this possibility should be explored by carefully analysing a wider Type Ibn SN sample. A more detailed discussion on the variety of properties observed in Type Ibn SNe, including the study of the evolution of a range of observed parameters (e.g the velocity of the different line components), will be faced in a forthcoming paper (Pastorello et al. in preparation).

SN 2006jc and similar objects (e.g. SNe 1999cq and 2002ao), which we indicate as prototypical SNe Ibn, show very weak or even no evidence of H in the CSM (Matheson et al. 2000; Pastorello et al. 2007; Foley et al. 2007; Pastorello et al. 2008a). This points toward progenitors that have lost most of their He-rich external layers, and were stripped of their H envelopes a long time before their CC SN explosion. This would therefore connect SN 2006jc to WN or even WCO progenitors (Tominaga et al. 2008). In this context, SN 2010al shows some differences. The early-time spectrum was dominated by a blue continuum, relatively prominent Balmer features, He II lines with $v_{FWHM} \approx$ 2250 km s^{-1}, and there was evidence for the presence of lines of CNO processing material (in particular the blend of N III λ4640 and C III λ4648, see Section 4.1). Such lines have been seen in the CSM of the Type IIn SNe 1998S (Fassia et al. 2001; Fransson et al. 2005) and 2008fq (Taddia et al. 2013), and considered indicative of CNO-element enrichment in the circumstellar wind produced by the progenitor star. This

[13] A narrow Hα has been detected in the spectra of iPTF13beo, but attibuted to galaxy background (Gorbikov et al. 2014).

[14] We note that Smith et al. (2012) cast some doubts on the membership of SN 2005la in the Type Ibn SN family, because of the slightly different shape of the continuum and the different line ratios. This was because SN 2005la still showed quite strong H lines in the spectrum, together with He lines. However, the H/He ratio shown by SN 2005la is very unusual for a Type IIn SN. In addition, the FWHM velocities of the He I lines ($\sim$ a few $\times$ 10^3 km s^{-1}, Pastorello et al. 2008b) are closer to those expected in WR winds rather then those one can find in typical LBV winds (Abbott & Conti 1987; Humphreys & Davidson 1994).

suggested enhanced mixing from the inner CNO burning regions to the outer layers, possibly favoured by stellar rotation. In the case of SN 2010al, the identified circumstellar lines and their velocities (exceeding 10^3 km s^{-1}) are well consistent with what expected in winds of WR stars.

A few days later, the spectrum of SN 2010al experienced a significant evolution, showing marginal or no evidence of He II and CNO element lines. It was instead characterized by narrow lines of He I (with an expansion velocity of about 1000 km s^{-1} from the position of the P-Cygni absorption minimum), whilst there was only a marginal evidence for the presence of Hα. At later epochs the spectra displayed the characteristic blue pseudo-continuum that is observed in SNe Ibn (and other interacting SNe), with the He I features showing a broader P-Cygni profile. The FWHM velocity of the He I increased to about 5-6 $\times$ 10^3 km s^{-1}, and became comparable with that measured for the strong Ca II and O I lines. Since these α-element lines are believed to form in the SN ejecta, this is probably an indication that a significant amount of He was still present in the pre-SN stellar envelope. In other words, the pre-SN star was probably still He-rich at the time of the collapse of the core. This links SN 2010al to more canonical type Ib SNe. The similarity with SNe Ib can also be noticed in the early photometric evolution of SN 2010al: the overall light curve shape is reminiscent of those of normal SNe Ib[15], although with a much wider post-peak magnitude drop ($\Delta M \sim 5$ mag in about 40 days). This would suggest that the luminosity from ejecta-CSM interaction contributes mostly to the very luminous light curve peak.

A plausible explanation for the evolution of the He I lines is that it is determined by the properties of the CSM: evidence of the underlying SN ejecta can be inferred from the apparent broadening of the He I lines that would be indicative of the growing emission contribution from the shocked ejecta. In this context, it is relevant here to discuss the outcomes of the X-ray observations (0.2-10 keV) of a sample of interacting SNe presented by Ofek et al. (2013), since three Type Ibn (including the two objects presented in this paper) were included in the SN sample of Ofek et al. They found that two Type Ibn SNe (SN 2006jc and 2010al) had very similar peak X-ray luminosities ($L_X \approx 2 \times 10^{41}$ erg s^{-1}), whilst for SN 2010hw they inferred an upper luminosity limit $L_X < 5 \times 10^{40}$ erg s^{-1}. In most cases of interacting SNe, the X-ray emission arises from the diffusion of shock breakout energy in a circumstellar shell. However, this explanation does not match the case of SN 2010al. Usually, in fact, the intensity of the X-ray emission from shock breakout energy diffusion is lower than that originating from ejecta-CSM interaction. In addition, Ofek et al. (2013) determined a surprisingly high L_X/L_{opt} ratio for SN 2010al, about 0.3, which is one order of magnitude higher than that measured for SN 2006jc (and about 2 orders of magnitude more than that estimated for SN 2011hw). Finally, the maximum of the L_X light curve is reached quite early (about 15 days from the optical maximum estimated to occur on JD = 2455284.3).[16] All of this makes implausible the shock breakout-CSM scenario for SN 2010al. More plausible is that the high X-ray emission of SN 2010al is determined by the conversion of a large fraction of kinetic energy into radiation, via shock-interaction of the SN ejecta with a circumstellar shell expelled a short time before the SN explosion. We remark that in coincidence with the peak of X-ray emissivity, the optical spectrum changes significantly, and becomes dominated by intermediate-width features.

In the case of SN 2011hw, the spectra show a variety of lines with multi-component profiles, and clear evidence of narrow, high-ionization forbidden Fe lines (Smith et al. 2012). These are signatures that high-frequency radiation ionizes the outer unshocked CSM. Taking into account the peculiar, non-linear decline of the optical light curve of SN 2011hw, the implication is that the SN ejecta interact with a CSM having a rather complex density profile and this likely powers the evolution of SN 2011hw for a longer period than for SN 2010al. We note that structured density profiles are quite common in the CSM of interacting SNe (see, e.g., Zampieri et al. 2005).

The spectral and photometric properties of SN 2010al indicate that the best scenario for this object is that of a Type Ib SN exploded in a He-rich, H-poor CSM. This implies that the progenitor star was totally H-stripped, and exploded while it was still losing the residual He-rich layers. The best candidate precursor of this SN is a WR star (probably a WN Type). The observables of SN 2011hw, on the other hand, collocate this object as a transitional event between a Type IIn SN and a Type Ibn SN. We agree with the conclusions of Smith et al. (2012) that the precursor of SN 2011hw was a post-LBV star, possibly an Ofpe/WN9 star, with some residual H in the envelope. In this sense the two objects may represent the extremes of the Type Ibn SN variety, and -with other Type Ibn events (see Table 4 in Pastorello et al. 2015a, for a comprehensive list)- they contribute to fill the *observational* gap between Type IIn and stripped-envelope SNe.

The Type Ibn SNe analyzed so far confirm that they are produced by WR stars, and the collapse of the stellar core may occasionally be heralded by major mass-loss events occurring a short time before the terminal SN explosion, as directly observed in SN 2006jc. The heterogeneity in the observed parameters of SNe Ibn are likely related to the different physical, geometrical and chemical properties of the CSM. This possibly results from different evolutionary paths for Type Ibn SN progenitors, implying that stars with a range of initial masses may reach different stages in the post-LBV stellar evolution toward a stripped C-O core.

ACKNOWLEDGMENTS

AP thanks Elia Cozzi, Rafael Benavides & Joseph Brimacombe for kindly providing their observations of SN 2010al

[15] SN 1999cq, here taken as representative for typical SNe Ibn, showed a rather asymmetric light curve with a very sharp rise to maximum and a relatively fast decline in the optical bands. OGLE-2012-SN006 (Pastorello et al. 2015b) had a photometric evolution similar to that of SN 2010al in the pre-maximum phase and during the first month past maximum. However, later on, the light curve of OGLE-2012-SN006 significantly flattened. This behaviour has never been observed in Type Ibn SNe before.

[16] We note that the epoch of the optical maximum for SN 2010al computed in this paper is over 2 weeks later than that assumed in the Ofek et al. (2013) paper (JD = 2455268.5).

for this study, and M. L. Pumo for useful discussions. We would like to thank the anonymous referee for providing us with constructive comments and suggestions.

AP, EC, SB, MLP, AH, LT, and MT are partially supported by the PRIN-INAF 2011 with the project Transient Universe: from ESO Large to PESSTO. DYT is partly supported by the Russian Foundation for Basic Research (project No. 13-02-92119). FB acknowledges support from FONDECYT through Postdoctoral grant 3120227 and by the Millennium Center for Supernova Science through grant P10-064-F (funded by Programa Bicentenario de Ciencia y Tecnología de CONICYT and Programa Iniciativa Científica Milenio de MIDEPLAN). ST acknowledges support by the Transregional Collaborative Research Centre TRR 33 of the German Research Foundation. MDS gratefully acknowledges generous support provided by the Danish Agency for Science and Technology and Innovation realized through a Sapere Aude Level 2 grant. XW is supported by the Major State Basic Research Development Program (2013CB834903), the National Natural Science Foundation of China (NSFC grants 11073013, 11178003, 11325313), and the Foundation of Tsinghua University (2011Z02170) This work is supported in part under grant number 1108890 from the US National Science Foundation and is partly supported by the European Union FP7 programme through ERC grant number 320360. This material is based upon work supported by NSF under grants AST–0306969, AST–0607438 and AST–1008343.

The MASTER network has made use of equipment acquired through the Development Program for Lomonosov Moscow State University, and was also supported by a grant in the form of a subsidy from the Ministry of Education and Science of the Russian Federation (agreement of August 27, 2012, No. 8415) and by the Dinastiya Foundation for Non-Commercial Programs. The work is supported by the Russian Foundation of Fundamental Research, grant RFFI 14-02-31546.

This work is partially based on observations of the European supernova collaboration involved in the ESO-NTT large programme 184.D-1140 led by Stefano Benetti. It is also based on observations made with ESO VLT Telescopes at the Paranal Observatory under program IDs 084.D-0265 and 085.D-0701 (PI. S. Benetti). The manuscript includes data obtained at the Large Binocular Telescope of the Mount Graham International Observatory. The LBT is an international collaboration among institutions in the United States, Italy and Germany. LBT Corporation partners are: The University of Arizona on behalf of the Arizona university system; Istituto Nazionale di Astrofisica, Italy; LBT Beteiligungsgesellschaft, Germany, representing the Max-Planck Society, the Astrophysical Institute Potsdam, and Heidelberg University; The Ohio State University, and The Research Corporation, on behalf of The University of Notre Dame, University of Minnesota and University of Virginia.

This paper is based on observations made with the Italian Telescopio Nazionale Galileo (TNG) operated on the island of La Palma by the Fundación Galileo Galilei of the INAF (Istituto Nazionale di Astrofisica). It is also based on observations made with the Liverpool Telescope (LT) operated on the island of La Palma at the Spanish Observatorio del Roque de los Muchachos of the Instituto de Astrofisica de Canarias; the William Herschel Telescope (WHT) operated on the island of La Palma by the Isaac Newton Group in the Spanish Observatorio del Roque de los Muchachos of the Instituto de Astrofsica de Canarias; the Nordic Optical Telescope (NOT), operated on the island of La Palma jointly by Denmark, Finland, Iceland, Norway, and Sweden, in the Spanish Observatorio del Roque de los Muchachos of the Instituto de Astrofísica de Canarias; the 0.80m Tsinghua-NAOC Telescope (TNT) in the Xinglong Observatory of NAOC; the 2.2m Telescope of the Centro Astronómico Hispano Alemán (CAHA) at Calar Alto, operated jointly by the Max-Planck Institut für Astronomie and the Instituto de Astrofísica de Andalucía (CSIC); the 1.82m Copernico Telescope and the 67/92-cm Schmidt Telescope of the INAF-Asiago Observatory; the 2-m Faulkes Telescope North at Haleakala Observatory (Hawaii, US). This work makes use of observations from the LCOGT network.

This publication makes use of data products from the Two Micron All Sky Survey, which is a joint project of the University of Massachusetts and the Infrared Processing and Analysis Center/California Institute of Technology, funded by the National Aeronautics and Space Administration and the National Science Foundation.

REFERENCES

Abbott, D. C., Conti, P. S. 1987, ARAA, 25 113
Anupama, G. C. et al. 2009, MNRAS, 392, 894
Benetti, S. et al. 2011, MNRAS, 411, 2726
Bianco, F. B. et al. 2014, ApJS, 213, 19
Bufano, F. et al. 2009, ApJ, 700, 1456
Breeveld, A. A. et al. 2011, in *Gamma-Ray Bursts 2010*, AIP Conference Proceedings, Volume 1358, pp. 373-376
Brown, P. J. et al. 2009, ApJ, 137, 4517
Chugai, N. N. 2009, MNRAS, 400, 866
Cooke, J. et al. 2010, Astron. Telegram 2491
Di Carlo, E. et al. 2008, ApJ, 684, 471
Dintinjana, B. et al. 2011, CBET 2906
Fassia, A. et al. 2001, MNRAS, 325, 907
Foley, R. J. et al. 2007, ApJ, 657, L105
Fransson, C. et al. 2002, ApJ, 572, 350
Fransson, C. et al. 2005, ApJ, 622, 991
Galama, T. J. et al. 1998, Nature, 395, 670
Gal-Yam, A. et al. 2007, ApJ, 656, 372
Gorbikov, E. et al. 2014, MNRAS, 443, 671
Groh, J. H., Maynet, G., Ekström, S. 2013, A&A, 550, L7
Groh, J. H., Maynet, G., Georgy, C., Ekström, S. 2013, A&A, 558, 131
Humphreys, R. M., Davidson, K. 1994, PASP, 106, 1025
Immler, S. et al. 2008, ApJ, 674, L85
Kaiser, N. et al. 2002, in *Survey and Other Telescope Technologies and Discoveries*, Proceedings of the SPIE, Volume 4836, pp. 154-164
Kargas, T. et al. 2013, Astron. Telegram 5380
Kiewe, M. et al. 2012, ApJ, 744, 10
Kirshner, R. et al. 2010, Astron. Telegram 2513
Kornilov, V. G. et al. 2012, Experimental Astronomy, 33, 173
Kotak, R., Vink, J. S. 2006, A&A, 460, L5
Kulkarni, S. R. 2013, Astron. Telegram, 4807, 1
Landolt, A. U. 1992, AJ, 104, 340

Lipunov, V. et al. 2010, Advances in Astronomy, 2010, article id. 349171
Matheson, T. et al. 2000, AJ, 119, 2303
Mattila, S. et al. 2008, MNRAS, 389, 141
McKenzie, E. H., Schaefer, B. E. 1999, PASP, 111, 964
Modjaz, M. et al. 2014, AJ, 147, 99
Nozawa, T. et al. 2008, ApJ, 684, 1343
Ofek et al. 2013, ApJ, 763, 42
Pastorello, A., Aretxaga, I., Zampieri, L., Mucciarelli, P., Benetti, S. 2005 in *1604-2004: Supernovae as Cosmological Lighthouses*, ASP Conference Series, Vol. 342, Proceedings of the conference held 15-19 June, 2004 in Padua, Italy. Edited by M. Turatto, S. Benetti, L. Zampieri, and W. Shea. San Francisco: Astronomical Society of the Pacific, p.285
Pastorello, A. et al. 2007, Nature, 447, 829
Pastorello, A. et al. 2008a, MNRAS, 389, 113
Pastorello, A. et al. 2008b, MNRAS, 389, 131
Pastorello, A. et al. 2009, MNRAS, 394, 2266
Pastorello, A. et al. 2012, Astron. Nachrichten, 332, 266
Pastorello, A. et al. 2015a MNRAS, accepted (eprint arXiv: submit/1186334)
Pastorello, A. et al. 2015b MNRAS, accepted (eprint arXiv: submit/1186313)
Patat, F. et al. 2001, ApJ, 555, 900
Poole, T. S. et al. 2008, MNRAS, 383, 627
Prieto, J. L., Morrell, N. 2013, Astron. Telegram 4734
Pritchard, T. A., Roming, P. W. A., Brown, P. J, Bayless, A. J., Frey, L. H. 2014, ApJ, 787, 157
Rabinowitz, D. et al. 2011, ApJ, 732, 512
Rich, D. 2010, CBET 2207
Roming, P. W. A. et al. 2005, SSRv, 120, 95
Sanders, N. E. et al. 2013, ApJ, 769, 39
Sakon, I. et al. 2009, ApJ, 692, 546
Schlafly, E. F., Finkbeiner, D. P. 2011, ApJ, 737, 103
Silverman, J. M. et al. 2010, CBET 2223
Skrutskie, M. F. et al. 2009, AJ, 131, 1163
Smith, N., Owocki, S. P. 2006, ApJ, 645, L45
Smith, N., Foley, R. J., Filippenko, A. V. 2008, ApJ, 680, 568
Smith, N. et al. 2009, ApJ, 695, 1334
Smith, N. et al. 2012, MNRAS, 426, 1905
Sollerman, J. et al. 2002, A&A, 386, 944
Sollerman, J. et al. 2013, Astron. Telegram 4731
Srivastav, S., Anupama, G. C., Sahu, D. K. 2014, MNRAS, 445, 1932
Stritzinger, M. et al. 2010, CBET 2220
Stritzinger, M. et al. 2012, ApJ, 756, 173
Taddia, F. et al. 2013, A&A, 555, 10
Tominaga, N. et al. 2008, ApJ, 687, 1208
Trundle, C., Kotak, R., Vink, J. S., Meikle, W. P. S. 2008, A&A, 483, L47
Trundle, C., et al. 2009, A&A, 504, 945
Turatto, M., Cappellaro, E., Danziger, I. J., Benetti, S., Gouiffes, C., della Valle, M. 1993, MNRAS, 262, 128
Valenti, S. et al. 2008, MNRAS, 383, 1485
Valenti, S. et al. 2011, CBET 2906, 2
Valenti, S. et al. 2012, Astron. Telegram 4037
Wyrzykowski, L., Udalski, A., Kozlowski, S. 2012, Astron. Telegram 4495
Zampieri, L. et al. 2005, MNRAS, 364, 1419

APPENDIX A: PHOTOMETRY TABLES

This paper has been typeset from a TEX/ LATEX file prepared by the author.

Table A1. Optical magnitudes of the sequences of local standards in the fields of SNe 2010al and 2011hw (Figure 1). The errors are the rms of the recovered magnitudes. If no error is indicated in brackets, the reported magnitude is that of a single (plausibly photometric) night.

SN 2010al					
Star	U	B	V	R	I
s1	–	18.09 (0.03)	17.45 (0.04)	17.01 (0.07)	16.43 (0.07)
s2	13.69	13.72 (0.03)	13.17 (0.03)	12.85 (0.07)	12.49 (0.07)
s3	–	–	18.44 (0.14)	17.85 (0.07)	–
s4	–	19.77 (0.11)	18.48 (0.09)	17.58 (0.02)	16.77 (0.02)
s5	13.40 (0.07)	13.48 (0.03)	13.02 (0.02)	12.80 (0.06)	12.47 (0.02)
s6	–	–	19.79 (0.07)	18.47 (0.02)	17.04 (0.02)
s7	16.12	15.86 (0.03)	15.07 (0.02)	14.66 (0.04)	14.24 (0.02)
s8	16.82 (0.05)	16.80 (0.03)	16.27 (0.02)	15.89 (0.02)	15.55 (0.05)
s9	16.80 (0.07)	16.15 (0.02)	15.25 (0.02)	14.76 (0.07)	14.21 (0.04)
s10	15.78 (0.03)	15.85 (0.03)	15.30 (0.03)	14.99 (0.04)	14.60 (0.04)
s11	15.50	15.50 (0.03)	14.86 (0.03)	14.48 (0.06)	14.09 (0.06)
s12	14.94	15.00 (0.03)	14.46 (0.03)	14.12 (0.07)	13.89 (0.09)
s13	15.96	15.40 (0.03)	14.54 (0.03)	14.02 (0.04)	13.57 (0.06)
s14	20.13	18.98 (0.03)	17.46 (0.02)	16.69 (0.06)	15.76 (0.05)
s15	17.32	17.35 (0.04)	16.84 (0.04)	16.50 (0.07)	16.07 (0.06)
s16	–	–	18.99 (0.07)	17.88 (0.07)	16.59 (0.07)
SN 2011hw					
Star	U	B	V	R	I
s1	12.82 (0.01)	12.69 (0.01)	12.08 (0.01)	11.73 (0.01)	11.39 (0.01)
s2	14.80 (0.01)	14.83 (0.01)	14.29 (0.01)	13.94 (0.01)	13.58 (0.01)
s3	15.32 (0.02)	15.22 (0.01)	14.51 (0.01)	14.09 (0.01)	13.68 (0.01)
s4	16.67 (0.02)	16.50 (0.01)	15.80 (0.02)	15.39 (0.01)	14.99 (0.01)
s5	–	16.04 (0.02)	15.36 (0.04)	14.85 (0.05)	14.50 (0.04)
s6	15.43 (0.01)	15.42 (0.01)	14.81 (0.01)	14.43 (0.01)	14.07 (0.01)
s7	16.64 (0.01)	16.44 (0.01)	15.73 (0.01)	15.29 (0.01)	14.89 (0.01)
s8	16.84 (0.03)	16.73 (0.01)	16.08 (0.02)	15.70 (0.02)	15.33 (0.01)
s9	17.69 (0.03)	17.19 (0.02)	16.32 (0.01)	15.83 (0.01)	15.36 (0.01)

Table A2. Swift/UVOT UV-bands magnitudes of the reference stars in the fields of SNe 2010al and 2011hw. The errors are the rms of the recovered magnitudes.

SN 2010al						
Star	$uvw2$	$uvm2$	$uvw1$	u	b	v
s5	15.24 (0.03)	14.94 (0.03)	14.23 (0.03)	–	–	–
s7	19.20 (0.14)	19.98 (0.21)	17.55 (0.08)	16.01 (0.05)	15.73 (0.04)	15.02 (0.04)
s8	19.44 (0.15)	19.38 (0.15)	18.03 (0.10)	16.84 (0.07)	16.79 (0.05)	16.27 (0.07)
s9	19.70 (0.19)	–	18.34 (0.12)	16.67 (0.07)	16.17 (0.04)	15.30 (0.04)
s10	18.15 (0.08)	17.94 (0.07)	16.88 (0.06)	15.70 (0.04)	15.78 (0.03)	15.36 (0.05)
s11	18.08 (0.09)	17.95 (0.08)	16.63 (0.06)	15.37 (0.04)	15.39 (0.03)	14.90 (0.04)
s12	16.99 (0.06)	16.66 (0.05)	15.88 (0.05)	14.83 (0.04)	14.94 (0.03)	14.51 (0.04)
s13	19.08 (0.13)	20.02 (0.22)	17.46 (0.08)	15.78 (0.05)	15.33 (0.03)	14.56 (0.04)
s15	19.76 (0.19)	19.45 (0.16)	18.49 (0.13)	17.27 (0.09)	17.32 (0.07)	16.81 (0.09)
SN 2011hw						
Star	$uvw2$	$uvm2$	$uvw1$	u	b	v
s1	15.73 (0.03)	15.88 (0.03)	14.16 (0.03)	12.77 (0.03)	12.74 (0.03)	12.12 (0.02)
s2	17.23 (0.04)	16.93 (0.04)	15.87 (0.03)	14.73 (0.04)	14.81 (0.02)	14.30 (0.03)
s3	18.31 (0.06)	18.61 (0.07)	16.70 (0.04)	15.26 (0.04)	15.17 (0.03)	14.52 (0.04)
s4	19.64 (0.12)	20.01 (0.16)	17.99 (0.07)	16.59 (0.04)	16.48 (0.02)	15.83 (0.04)
s5	19.38 (0.11)	20.14 (0.17)	17.82 (0.06)	16.25 (0.05)	16.08 (0.03)	15.35 (0.03)
s6	18.27 (0.06)	18.23 (0.06)	16.74 (0.04)	15.39 (0.04)	15.41 (0.02)	14.84 (0.03)
s7	19.69 (0.13)	20.04 (0.17)	18.13 (0.07)	16.62 (0.05)	16.47 (0.03)	14.79 (0.03)
s8	19.69 (0.13)	19.60 (0.12)	18.12 (0.07)	16.78 (0.05)	16.71 (0.03)	16.11 (0.04)

Table A3. Calibrated photometry of SN 2010al. The errors in brackets are obtained by combining in quadrature the errors in the photometric calibration and instrumental PSF measurement errors. The symbol "*" marks unfiltered data rescaled to the R-band magnitudes; the symbol "†" indicates luminance filter measurements reported to V-band magnitudes. Standard Johnson-Cousins V- and R-band magnitudes from amateur astronomers have been obtained by computing instrumental zeropoints using the V and R magnitudes of the local sequence stars reported in Table A1, and adopting no colour correction. The numbers in the last column identify the intrumental configurations (see table footnotes). A relative uncertainty of 10 per cent on the flux calibration has been assumed for the VLT spectra.

Date	JD +2455000	U	B	V	R	I	J	H	K	Source
07Feb10*	234.64	–	–	–	>19.83	–	–	–	–	1
12Mar10	268.21	–	–	–	>19.16	–	–	–	–	2
13Mar10*	268.53	–	–	–	18.87 (0.24)	–	–	–	–	1
15Mar10*	271.39	–	–	–	17.65 (0.27)	–	–	–	–	3
16Mar10*	271.57	–	–	–	17.57 (0.25)	–	–	–	–	1
16Mar10†	271.93	–	–	17.34 (0.13)	–	–	–	–	–	4
16Mar10	271.95	–	–	–	17.35 (0.32)	–	–	–	–	5
16Mar10†	272.01	–	–	17.33 (0.10)	–	–	–	–	–	4
16Mar10	272.43	–	–	–	17.00 (0.08)	–	–	–	–	2
17Mar10*	272.54	–	–	–	16.94 (0.19)	–	–	–	–	1
17Mar10	272.97	–	16.77 (0.09)	16.97 (0.06)	16.77 (0.08)	16.70 (0.08)	–	–	–	6
17Mar10	273.01	–	–	–	16.75 (0.12)	–	–	–	–	5
17Mar10	273.39	–	–	–	16.71 (0.10)	–	–	–	–	2
18Mar10*	273.50	–	–	–	16.66 (0.09)	–	–	–	–	1
18Mar10	274.19	–	–	–	16.46 (0.05)	–	–	–	–	2
19Mar10	275.06	–	–	–	16.23 (0.10)	–	–	–	–	5
19Mar10	275.21	–	–	–	16.25 (0.05)	–	–	–	–	2
20Mar10	276.36	–	–	–	15.98 (0.06)	–	–	–	–	2
21Mar10	277.23	–	–	–	16.00 (0.06)	–	–	–	–	2
22Mar10	278.25	–	–	–	15.74 (0.02)	–	–	–	–	2
23Mar10	279.49	–	–	–	–	–	15.35 (0.42)	15.32 (0.50)	–	7
25Mar10	280.55	15.08 (0.12)	15.91 (0.12)	15.83 (0.12)	15.72 (0.12)	15.66 (0.12)	15.33 (0.12)	15.19 (0.12)	15.05 (0.12)	8
26Mar10	282.04	–	–	15.84 (0.06)	15.69 (0.09)	–	–	–	–	6
26Mar10	282.11	–	15.93 (0.05)	15.84 (0.06)	15.71 (0.04)	15.63 (0.08)	–	–	–	6
27Mar10	282.50	–	–	–	–	–	15.31 (0.45)	15.18 (0.31)	–	7
27Mar10*	282.60	–	–	–	15.63 (0.05)	–	–	–	–	1
27Mar10	283.08	–	15.95 (0.15)	15.85 (0.06)	15.70 (0.05)	15.57 (0.06)	–	–	–	6
28Mar10	283.97	–	15.95 (0.14)	15.82 (0.07)	15.66 (0.08)	15.53 (0.12)	–	–	–	6
28Mar10	283.99	–	–	–	15.56 (0.11)	–	–	–	–	5
29Mar10	284.50	15.21 (0.12)	15.93 (0.12)	15.80 (0.12)	15.70 (0.12)	15.57 (0.12)	15.46 (0.12)	15.33 (0.12)	15.37 (0.12)	8
02Apr10*	289.44	–	–	–	15.65 (0.07)	–	–	–	–	9
04Apr10	291.37	–	–	–	–	–	15.77 (0.38)	15.34 (0.32)	–	7
05Apr10*	291.57	–	–	–	15.77 (0.07)	–	–	–	–	1
06Apr10	292.97	–	–	–	15.94 (0.08)	–	–	–	–	5
06Apr10	292.99	–	16.44 (0.05)	16.13 (0.08)	15.92 (0.05)	15.68 (0.07)	–	–	–	6
06Apr10	293.45	–	16.47 (.11)	16.13 (0.06)	15.92 (0.09)	15.72 (0.08)	–	–	–	10
07Apr10	294.49	15.95 (0.12)	16.47 (0.12)	16.18 (0.12)	16.03 (0.12)	15.80 (0.12)	15.76 (0.12)	15.49 (0.12)	15.16 (0.12)	8
11Apr10*	297.57	–	–	–	16.31 (0.06)	–	–	–	–	1
11Apr10	298.36	–	–	–	–	–	16.03 (0.24)	15.79 (0.22)	–	7
14Apr10	300.99	–	17.35 (0.08)	16.83 (0.08)	16.56 (0.06)	16.20 (0.07)	–	–	–	6
17Apr10	303.55	17.85 (0.12)	17.94 (0.05)	17.43 (0.05)	17.03 (0.07)	16.62 (0.05)	–	–	–	11
19Apr10	305.61	–	–	–	–	–	16.76 (0.12)	16.77 (0.18)	16.49 (0.14)	12
22Apr10	309.36	–	–	–	–	–	16.98 (0.40)	16.96 (0.28)	–	7
25Apr10	312.38	–	–	–	–	–	17.58 (0.45)	17.33 (0.46)	–	7
30Apr10	316.67	–	>18.58	19.36 (0.32)	–	–	–	–	–	6
01May10*	317.54	–	–	–	18.76 (0.31)	–	–	–	–	1
05May10	321.41	20.46 (0.36)	20.24 (0.09)	19.68 (0.10)	19.29 (0.15)	18.76 (0.14)	–	–	–	13
11May10	328.49	20.94 (0.12)	20.92 (0.12)	20.31 (0.12)	20.16 (0.12)	19.87 (0.12)	19.33 (0.12)	18.65 (0.12)	18.36 (0.12)	8
14Sep10	453.68	–	>22.29	>22.15	>21.55	>21.19	–	–	–	14
11Oct10	481.00	–	–	–	–	–	20.34 (0.14)	19.64 (0.12)	19.60 (0.23)	15
26Oct10	495.58	>19.00	>20.59	>19.28	>19.20	>19.68	–	–	–	14
02Jan11	563.64	>19.98	>20.12	>20.06	>19.87	>19.49	–	–	–	11
31Jan11	592.65	–	–	–	–	–	>20.41	>19.74	–	15
31Mar11	651.63	–	–	–	–	–	>19.50	–	>17.55	15

1 = Meade 16" Reflector + SBIG ST-9XE Dual CCD camera (Rich Observatory, Hampden, Maine, USA; obs. D.R.); 2 = 0.4-m MASTER telescope + Apogee Alta U16M CCD (Kislovodsk, Caucasian region Russia); 3 = 0.36-m Schmidt-Cassegrain + Apogee ALTA U47 CCD camera (New Millennium Observatory, Mozzate, Italy; obs. E. Cozzi); 4 = 12.5-inch RCOS Telescope + SBIG STL6303 CCD camera (Macedon Ranges Observatory, Melbourne, Australia; obs. J. Brimacombe); 5 = 0.4-m MASTER Telescope + Apogee Alta U16M CCD (Blagoveschensk; Far East region, Russia); 6 = 0.80-m Tsinghua-NAOC Telescope + Princeton Instruments VersArray:1300B CCD (Xinglong Observatory, Yanshan mountains, Hebei, China). 7 = 2.0-m Liverpool Telescope + SupIRCam (La Palma, Canary Islands, Spain); 8 = 8.2-m Very Large Ttelescope (UT2) + XShooter (spectro-photometry; European Southern Observatory; Cerro Paranal, Chile); 9 = 280-mm Celestron 11 + Atik 16HR with Sony chip ICX285AL (Posadas Observatory; Còrdoba, Spain; obs. R. Benavides); 10 = 1.82-m Copernico Telescope + AFOSC (Mt. Ekar, Asiago, Italy); 11 = 3.58-m New Technology Telescope + EFOSC2 (European Southern Observatory; La Silla, Chile); 12 = 3.58-m New Technology Telescope + SOFI (European Southern Observatory; La Silla, Chile); 13 = 3.58-m Telescopio Nazionale Galileo + Dolores (La Palma, Canary Islands, Spain); 14 = 2.2-m Calar Alto Telescope + CAFOS (Calar Alto Observatory, Almerìa, Spain); 15 = 2 × 8.4-m Large Binocular Telescope + Lucifer (Mt. Graham International Observatory, Arizona, USA);

Table A4. Table with the calibrated multi band photometry of SN 2011hw. The errors in brackets are obtained by combining in quadrature the errors of the photometric calibration and the instrumental PSF measurement errors. The symbol "*" indicates unfiltered measurements rescaled to R-band magnitudes. These have been obtained by computing zeropoints using the R-band magnitudes of the stellar sequence in the SN field, and assuming negligible colour correction.

Date	JD+2455000	U	B	V	R	I	Source
19Nov11	885.27	–	16.99 (0.02)	16.86 (0.03)	16.60 (0.02)	16.31 (0.03)	1
20Nov11	886.32	16.47 (0.02)	17.00 (0.03)	16.85 (0.04)	16.62 (0.04)	16.30 (0.05)	1
21Nov11	887.29	–	17.05 (0.12)	16.85 (0.19)	16.68 (0.14)	16.31 (0.18)	2
22Nov11	888.24	–	17.14 (0.02)	16.87 (0.09)	16.68 (0.05)	16.37 (0.07)	2
23Nov11	889.30	–	17.15 (0.04)	16.87 (0.05)	16.71 (0.13)	16.36 (0.14)	2
24Nov11	890.46	–	17.12 (0.08)	16.92 (0.19)	16.81 (0.17)	16.42 (0.26)	1
27Nov11	893.25	16.57 (0.02)	17.11 (0.06)	16.99 (0.04)	16.76 (0.10)	16.41 (0.04)	1
29Nov11	895.39	16.55 (0.03)	17.11 (0.02)	16.98 (0.02)	16.77 (0.02)	16.32 (0.03)	3
10Dec11	905.72	16.19 (0.04)	16.90 (0.04)	16.76 (0.05)	16.58 (0.04)	16.21 (0.07)	4
11Dec11	907.37	16.21 (0.03)	16.89 (0.02)	16.79 (0.02)	16.65 (0.02)	16.27 (0.02)	5
17Dec11	912.76	16.50 (0.04)	17.02 (0.03)	16.83 (0.01)	16.65 (0.05)	16.34 (0.08)	4
17Dec11	913.39	16.60 (0.02)	17.08 (0.03)	16.90 (0.02)	16.71 (0.02)	16.39 (0.02)	6
18Dec11*	914.26	–	–	–	16.71 (0.16)	–	1
21Dec11	917.34	16.92 (0.03)	17.35 (0.01)	17.06 (0.01)	16.96 (0.01)	16.52 (0.01)	7
22Dec11	917.76	16.81 (0.06)	17.34 (0.03)	17.07 (0.05)	16.97 (0.07)	16.56 (0.08)	4
23Dec11	919.26	16.98 (0.03)	17.37 (0.03)	17.20 (0.02)	17.08 (0.03)	16.55 (0.07)	3
26Dec11	922.36	17.03 (0.06)	17.58 (0.02)	17.30 (0.03)	17.29 (0.02)	16.90 (0.02)	5
29Dec11	924.73	17.29 (0.05)	17.70 (0.03)	17.37 (0.04)	17.31 (0.02)	16.98 (0.04)	4
01Jan12	928.27	–	17.91 (0.03)	17.64 (0.02)	17.56 (0.02)	17.03 (0.04)	3
04Jan12	931.27	–	18.05 (0.32)	17.76 (0.30)	17.69 (0.17)	17.28 (0.29)	2
05Jan12	932.35	17.90 (0.18)	18.24 (0.07)	17.83 (0.04)	17.78 (0.04)	17.41 (0.04)	5
10Jan12	937.24	–	18.36 (0.24)	18.03 (0.24)	18.14 (0.16)	17.51 (0.29)	2
12Jan12	939.33	–	18.49 (0.07)	18.18 (0.08)	18.19 (0.07)	17.54 (0.04)	3
17Jan12	944.23	18.65 (0.16)	–	18.47 (0.20)	18.44 (0.14)	17.82 (0.16)	1
17Jan12*	944.34	–	–	–	18.40 (0.28)	–	6
18Jan12*	945.35	–	–	–	18.48 (0.18)	–	6
18Jan12	945.37	–	19.00 (0.19)	18.48 (0.17)	–	–	1
21Jan12	948.22	19.01 (0.41)	18.97 (0.26)	18.58 (0.13)	18.59 (0.16)	17.95 (0.20)	1
27Jan12	954.24	–	19.45 (0.15)	19.08 (0.18)	18.95 (0.19)	18.57 (0.21)	1
30Jan12	957.22	–	19.92 (0.30)	19.35 (0.24)	19.34 (0.30)	18.58 (0.27)	1
25Jul12	1133.67	–	–	–	>23.16	>23.08	6
02Aug12	1141.55	–	–	>20.44	–	–	1
21Aug12	1160.60	>23.29	>23.85	>24.15	–	–	7

1 = 1.82m Copernico Telescope + AFOSC (Mt. Ekar, Asiago, Italy); 2 = 67/92-cm Schmidt Telescope + SCAM (Mt. Ekar, Asiago, Italy); 3 = 2.2-m Calar Alto Telescope + CAFOS (Calar Alto Obs., Almerìa, Spain); 4 = 2.0-m Faulkes Telescope North + EM03 (Haleakala, Hawaii Isl., USA); 5 = 2.0-m Liverpool Telescope + RATCam (La Palma, Canary Isl., Spain); 6 = 3.58-m Telescopio Nazionale Galileo + Dolores (La Palma, Canary Isl., Spain); 7 = 4.2-m William Herschel Telescope + ACAM (La Palma, Canary Isl., Spain).

Table A5. Table with the Swift/UVOT band photometry of SNe 2010al and 2011hw. Template subtraction was applied to the UVOT images of both SNe. Original u, b, v UVOT magnitudes have been converted to those in the Johnson-Cousins photometric system using the magnitudes of the stellar sequences reported in Table A1.

SN 2010al							
Date	JD+2455000	$uvw2$	$uvm2$	$uvw1$	u	b	v
23Mar10	279.27	14.64 (0.14)	14.60 (0.07)	14.58 (0.08)	–	–	–
28Mar10	284.38	16.06 (0.18)	15.61 (0.10)	15.33 (0.08)	15.06 (0.09)	15.98 (0.10)	15.80 (0.08)
30Mar10	286.05	16.32 (0.20)	15.97 (0.18)	15.56 (0.09)	15.22 (0.09)	16.07 (0.09)	15.86 (0.12)
01Apr10	288.06	16.68 (0.17)	16.52 (0.10)	15.86 (0.10)	15.30 (0.10)	16.12 (0.10)	15.81 (0.10)
03Apr10	289.87	17.13 (0.17)	16.93 (0.25)	16.12 (0.12)	15.46 (0.13)	16.26 (0.10)	15.89 (0.14)
05Apr10	291.74	17.61 (0.18)	17.55 (0.18)	16.73 (0.19)	15.72 (0.11)	16.33 (0.10)	16.08 (0.14)
07Apr10	293.72	18.01 (0.19)	17.85 (0.19)	16.93 (0.15)	15.78 (0.11)	16.51 (0.11)	16.20 (0.11)
09Apr10	295.96	18.35 (0.33)	18.36 (0.36)	17.48 (0.36)	16.15 (0.19)	16.76 (0.19)	16.28 (0.21)
11Apr10	297.81	18.87 (0.34)	18.57 (0.46)	17.86 (0.28)	16.58 (0.13)	16.91 (0.18)	16.54 (0.17)
13Apr10	299.73	19.22 (0.48)	18.88 (0.28)	18.18 (0.29)	16.82 (0.14)	17.12 (0.12)	16.72 (0.19)
17Apr10	304.26	>19.53	19.31 (0.38)	18.73 (0.31)	17.93 (0.29)	18.04 (0.20)	17.53 (0.22)
19Apr10	306.06	>19.48	>19.30	18.95 (0.33)	18.15 (0.33)	18.29 (0.28)	17.88 (0.30)
23Apr10	310.18	>19.44	>19.31	19.26 (0.37)	>18.49	18.92 (0.30)	>17.89
25Apr10	311.75	>19.33	>19.31	>18.64	>18.42	>18.85	>17.84
27Apr10	313.55	>19.45	>19.36	>18.69	>18.48	>18.92	>17.98
29Apr10	316.03	>19.63	>19.41	>18.78	>18.67	>19.03	>18.21
03May10	319.98	>19.46	>19.37	>18.82	>18.59	>18.81	>18.14
05May10	322.09	>19.32	>19.22	>18.79	>18.30	>18.58	>17.93
27Feb11	588.39	>19.46	>19.32	>18.62	>19.57	>18.79	>18.01
SN 2011hw							
Date	JD+2455000	$uvw2$	$uvm2$	$uvw1$	u	b	v
22Nov11	888.27	17.48 (0.06)	17.34 (0.07)	16.89 (0.07)	16.46 (0.06)	17.11 (0.07)	16.93 (0.09)
24Nov11	890.45	17.70 (0.07)	17.41 (0.07)	16.87 (0.07)	16.59 (0.07)	17.15 (0.07)	16.97 (0.09)
26Nov11	891.87	17.70 (0.07)	17.42 (0.07)	16.90 (0.07)	16.57 (0.07)	17.15 (0.07)	16.93 (0.09)
28Nov11	893.96	17.69 (0.07)	17.38 (0.07)	16.90 (0.07)	16.58 (0.07)	17.14 (0.08)	17.03 (0.10)
30Nov11	896.17	17.51 (0.07)	17.14 (0.07)	16.62 (0.06)	16.48 (0.06)	17.03 (0.07)	17.00 (0.09)
14Apr13	1397.24	>19.81	>19.67	>19.46	>19.00	>19.02	>18.34